J Eng Math (2010) 68:57–83
DOI 10.1007/s10665-009-9359-y

Fiber-reinforced hyperelastic solids: a realizable homogenization constitutive theory

Oscar Lopez-Pamies · Martín I. Idiart

Received: 2 July 2009 / Accepted: 19 December 2009 / Published online: 8 January 2010

Abstract A new homogenization theory to model the mechanical response of hyperelastic solids reinforced by a *random* distribution of aligned cylindrical fibers is proposed. The central idea is to devise a special class of microstructures—by means of an iterated homogenization procedure in finite elasticity together with an exact dilute result for sequential laminates—that allows to compute *exactly* the macroscopic response of the resulting fiber-reinforced materials. The proposed framework incorporates direct microstructural information up to the two-point correlation functions, and requires the solution to a Hamilton–Jacobi equation with the fiber concentration and the macroscopic deformation gradient playing the role of "time" and "spatial" variables, respectively. In addition to providing constitutive models for the macroscopic response of fiber-reinforced materials, the proposed theory also gives information about the local fields in the matrix and fibers, which can be used to study the evolution of microstructure and the development of instabilities. As a first application of the theory, *closed-form* results for the case of Neo-Hookean solids reinforced by a transversely isotropic distribution of anisotropic fibers are worked out. These include a novel explicit criterion for the onset of instabilities under general finite-strain loading conditions.

Keywords Finite strain · Hamilton–Jacobi equation · Homogenization · Instabilities · Microstructures

1 Introduction

Soft solids that are reinforced by stiff cylindrical fibers constitute an important class of technological and biological material systems. The classical example is that of tires. Other prominent examples of more recent interest include nano-structured thermoplastic elastomers [1,2] and biological tissues such as arterial walls [3] and ligaments [4].

O. Lopez-Pamies (✉)
Department of Mechanical Engineering, State University of New York, Stony Brook, NY 11794-2300, USA
e-mail: oscar.lopez-pamies@sunysb.edu

M. I. Idiart
Área Departamental Aeronáutica, Facultad de Ingeniería, Universidad Nacional de La Plata, Calles 1 y 47, La Plata B1900TAG, Argentina
e-mail: martin.idiart@ing.unlp.edu.ar

M. I. Idiart
Consejo Nacional de Investigaciones Científicas y Técnicas (CONICET), Avda. Rivadavia 1917, Cdad. de, Buenos Aires C1033AAJ, Argentina

Experimental evidence suggests that the macroscopic mechanical response of many among such classes of material systems is, to a first approximation, nonlinearly elastic. Making use of this simplifying assumption, there is a voluminous literature on *phenomenological* constitutive models for fiber-reinforced hyperelastic solids (see, e.g., [5–9]) that are based on the theory of transversely isotropic invariants (see, e.g., [10]). Using a different approach in which the local properties of the constituents (i.e., the matrix and the fibers) and the microstructure (i.e., the size, shape, and orientation of the fibers) are directly accounted for, there are also a number of recent *homogenization-based* constitutive models [11–14].

In this work, we propose a new homogenization strategy to derive constitutive models for fiber-reinforced hyperelastic solids. The key idea is to construct fiber-reinforced *random* microstructures that permit the exact computation of the macroscopic properties of the resulting material systems. More specifically, our approach, which closely follows that of Idiart [15] in the context of small-strain nonlinear elasticity, is comprised of two main steps. First, we derive an iterated dilute homogenization procedure in finite elasticity that provides, in the form of an initial-value problem, an exact result for the macroscopic stored-energy function of large classes of fiber-reinforced solids directly in terms of an auxiliary dilute problem. The second step deals with the formulation of the auxiliary dilute problem. It consists in devising a class of sequential laminates whose matrix phase is present in dilute concentrations, and whose macroscopic response can be computed explicitly. Sequential laminates of this sort were first considered in finite elasticity by deBotton [16].

In addition to generating constitutive models for the macroscopic response of fiber-reinforced hyperelastic solids, the formulation proposed in this work also grants access to the *local fields* in these material systems, which in turn permit a thorough study of the evolution of microstructure and the onset of instabilities. This feature is of the essence in the context of finitely deformable heterogeneous materials (see, e.g., [17, Sect. 2.5]). Indeed, since microstructural changes can result in dominant geometric softening/stiffening mechanisms, knowledge of the evolution of microstructure in fiber-reinforced hyperelastic solids (for instance, the rotation of the fibers) is critical to have complete insight into the macroscopic response of this class of materials. Moreover, given that instabilities are often the precursors of failure, knowledge of the onset of instabilities in fiber-reinforced hyperelastic solids, such as long and short wavelength instabilities, fiber failure, fiber debonding, and matrix cavitation, is crucial to understand the limits of applicability of the proposed macroscopic constitutive models.

The structure of the paper is organized as follows. First, in Sect. 2 we introduce some basic notation and set up the problem of the homogenization of two-phase fiber-reinforced hyperelastic solids. In Sect. 3, we derive the proposed homogenization constitutive theory. In particular, Sect. 3.1 is concerned with the iterated dilute homogenization procedure in finite elasticity, Sect. 3.2 deals with the auxiliary dilute problem of sequential laminates, and, finally, Sect. 3.3 presents the main result of this paper: the constitutive model for fiber-reinforced hyperelastic solids given by expression (33). Section 3.3 also includes the specialization of the proposed theory to incompressible constituents and transversely isotropic materials, cases of particular interest for application purposes. A general framework to study the evolution of microstructure from the local fields provided by the theory is put forward in Sect. 4. In Sect. 5, we discuss the onset of instabilities and derive a new explicit result for the onset of loss of strong ellipticity of a broad class of transversely isotropic stored-energy functions. Section 6 presents an application of the proposed general theory to the case of Neo-Hookean solids reinforced by a random and transversely isotropic distribution of anisotropic fibers. This includes *closed-form* results for the macroscopic stored-energy function and a novel failure criterion for general finite-strain loading conditions. We conclude the paper by recording some theoretical and practical remarks in Sect. 7.

2 Preliminaries on fiber-reinforced solids and homogenization

Fiber-reinforced materials are taken here to be made up of a continuous matrix phase containing aligned cylindrical fibers *randomly* distributed on the transverse plane and perfectly bonded to the matrix. We denote by Ω_0 the volume occupied by a representative specimen in the undeformed (reference) configuration, by $\partial\Omega_0$ the associated external boundary, and by the unit vector $\mathbf{N}$ the orientation of the fibers in the undeformed configuration. The interest is on

materials where the characteristic size of the cross-section of the fibers is much smaller than the size of the specimen and the scale of variation of the applied loads. It is further assumed that the random microstructure is statistically uniform and ergodic.

Both the matrix ($r = 1$) and the fibers ($r = 2$) are taken to be hyperelastic solids, characterized by non-convex, objective stored-energy functions $W^{(r)}$ of the deformation gradient $\mathbf{F}$. No further requirements on the functions $W^{(r)}$ are imposed at this point, except for the usual assumption that

$$W^{(r)}(\mathbf{F}) = \frac{1}{2}\boldsymbol{\varepsilon} \cdot \boldsymbol{\mathcal{L}}_0^{(r)}\boldsymbol{\varepsilon} + O\left(||\mathbf{F} - \mathbf{I}||^3\right), \tag{1}$$

in the limit as $\mathbf{F} \to \mathbf{I}$ for consistency with the classical theory of linear elasticity. In the above expression, $\boldsymbol{\varepsilon} = (\mathbf{F} + \mathbf{F}^T - 2\mathbf{I})/2$ is the infinitesimal strain tensor, and $\boldsymbol{\mathcal{L}}_0^{(r)}$ are positive definite fourth-order modulus tensors. At each material point $\mathbf{X}$ in the undeformed configuration, the first Piola–Kirchoff stress $\mathbf{S}$ is thus related to the deformation gradient $\mathbf{F}$ by

$$\mathbf{S} = \frac{\partial W}{\partial \mathbf{F}}(\mathbf{X}, \mathbf{F}), \quad W(\mathbf{X}, \mathbf{F}) = \sum_{r=1}^{2} \chi_0^{(r)}(\mathbf{X})\ W^{(r)}(\mathbf{F}), \tag{2}$$

where the $\chi_0^{(r)}$ are characteristic functions that take the value 1 if the position vector $\mathbf{X}$ is in phase r, and 0 otherwise, and serve to describe the microstructure in the undeformed configuration Ω_0.

In view of the microstructural randomness and cylindrical symmetry, the functions $\chi_0^{(r)}$ in (2) depend on the coordinate $\mathbf{X}$ only through its in-plane projection $\hat{\mathbf{X}}$, and are random variables that must be characterized in terms of ensemble averages [18]. Thus, the ensemble average of $\chi_0^{(r)}(\mathbf{X})$ represents the one-point probability $p_0^{(r)}(\mathbf{X})$ of finding phase r at $\mathbf{X}$; the ensemble average of the product $\chi_0^{(r)}(\mathbf{X})\chi_0^{(s)}(\mathbf{X}')$ represents the two-point probabilities $p_0^{(rs)}(\mathbf{X}, \mathbf{X}')$ of finding simultaneously phase r at $\mathbf{X}$ and phase s at $\mathbf{X}'$. Higher-order probabilities are defined similarly. Due to the assumed statistical uniformity and ergodicity, the one-point probability $p_0^{(r)}(\mathbf{X})$ can be identified with the initial volume fractions (or concentrations) $c_0^{(r)}$ of each phase r, while the two-point probabilities satisfy the relations

$$p_0^{(11)} - c_0^{(1)^2} = p_0^{(22)} - c_0^{(2)^2} = -\left(p_0^{(12)} - c_0^{(1)}c_0^{(2)}\right) = c_0^{(1)}c_0^{(2)}h, \tag{3}$$

for some even function h with $h(\mathbf{0}) = 1$ that depends on $(\hat{\mathbf{X}} - \hat{\mathbf{X}}')$ only, and contain information about the shape and distribution of the fibers. If, in addition, the random distribution of fibers over the cross-section has no long-range order, h tends to zero—usually with exponential decay—as $|\hat{\mathbf{X}} - \hat{\mathbf{X}}'| \to \infty$. As discussed in full detail in Sect. 3, the constitutive theory to be developed here incorporates information up to two-point statistics. We note, however, that the general procedure to be employed could be utilized, in principle, to develop theories that incorporate statistics of higher order.

Following Hill [19], we define the *macroscopic behavior* of the fiber-reinforced material as the relation between the average stress and the average deformation gradient over the entire specimen in the undeformed configuration. Formally, it can be characterized by

$$\overline{\mathbf{S}} = \frac{\partial \overline{W}}{\partial \overline{\mathbf{F}}}(\overline{\mathbf{F}}), \tag{4}$$

where

$$\overline{W}(\overline{\mathbf{F}}) = \min_{\mathbf{F} \in \mathcal{K}(\overline{\mathbf{F}})} \frac{1}{\Omega_0} \int_{\Omega_0} W(\mathbf{X}, \mathbf{F}) \mathrm{d}\mathbf{X}, \tag{5}$$

is the *effective stored-energy function*. In the above expressions, the overbar denotes averages over Ω_0, and $\mathcal{K}$ is the set of admissible deformation gradients:

$$\mathcal{K}(\overline{\mathbf{F}}) = \left\{\mathbf{F} | \exists \mathbf{x}(\mathbf{X}) \text{ with } \mathbf{F} = \partial \mathbf{x}/\partial \mathbf{X} \text{ and } \det \mathbf{F} > 0 \text{ in } \Omega_0, \mathbf{x} = \overline{\mathbf{F}}\mathbf{X} \text{ on } \partial\Omega_0\right\}. \tag{6}$$

Physically, the function $\overline{W}$ represents the average elastic energy stored in the specimen when subjected to an affine deformation on its boundary with average $\overline{\mathbf{F}}$. Moreover, from the definition (5) and the objectivity of the local functions $W^{(r)}$, it can be shown that $\overline{W}$ is an objective function of $\overline{\mathbf{F}}$. It is also noted that, by definition, $\overline{W}$ is quasi-convex, and therefore rank-one convex, but not strictly so, as discussed in more detail further below.

Because of the non-convexity of W in $\mathbf{F}$, the solution to the Euler–Lagrange equations associated with the variational problem (5) need *not* be unique. However, given the asymptotic quadratic behavior (1) of the local energies, the minimization (5) is expected[1] to yield a well-posed linearly elastic problem with a unique solution within a sufficiently small neighborhood of $\overline{\mathbf{F}} = \mathbf{I}$. As the deformation progresses beyond the linearly elastic neighborhood into the finite-deformation regime, the fiber-reinforced material may reach a point at which this "principal" solution bifurcates into different energy solutions. This point corresponds to the onset of an instability, beyond which the applicability of the "principal" solution becomes questionable. In this regard, it is useful to make the distinction between "macroscopic" instabilities, that is, geometric instabilities with wavelengths much larger than the characteristic size of the microstructure, and "local" instabilities, which include geometric instabilities with wavelengths that are comparable to the characteristic size of the microstructure, as well as material instabilities, such as loss of strong ellipticity and cavitation, of the local constituents. The computation of local instabilities requires knowledge of the entire deformation field $\mathbf{x}(\mathbf{X})$ that minimizes (5), and it is therefore a practically impossible task for random material systems. On the other hand, the computation of macroscopic instabilities is a much simpler endeavor, since it reduces to the detection of loss of strong ellipticity of the effective stored-energy function evaluated at the above-described "principal" solution [20]. In addition to providing feasible means to compute the onset of macroscopic instabilities, a further utility of the effective stored-energy function evaluated at the "principal" solution is that its loss of strong ellipticity provides an upper bound for the deformation levels at which any other instability (i.e., a local instability) may develop.[2]

In deriving tractable constitutive relations for heterogeneous hyperelastic solids, in view of the above remarks, it is thus common practice to neglect most (especially geometric) local instabilities and concentrate on macroscopic instabilities. Further justification for this practice has been provided by recent full-field simulations of particulate hyperelastic composites, which show that many local instabilities associated with periodic systems tend to disappear as the periodicity of the microstructure is broken down [21–23], thus suggesting that macroscopic instabilities may be the more relevant ones for random systems. Neglecting local instabilities amounts to considering an alternative definition of effective stored-energy function, formally given by

$$\overline{W}^{*}(\overline{\mathbf{F}}) = \min_{\mathbf{F}\in\mathcal{K}^{*}(\overline{\mathbf{F}})} \frac{1}{\Omega_0}\int_{\Omega_0} W(\mathbf{X},\mathbf{F})\mathrm{d}\mathbf{X}, \tag{7}$$

where the minimization is now over a suitably restricted set $\mathcal{K}^{*}$ of deformation gradient tensors that includes the above-described "principal" solution but excludes complicated bifurcation solutions associated with local instabilities. The precise choice of the set $\mathcal{K}^{*}$ depends on the specific material system of interest. Prominent examples of restricted sets are the set of uniform-per-layer fields commonly employed for layered solids (see, e.g., [16,24]), and the set of radially symmetric fields employed for solids with composite sphere assemblage microstructures subject to hydrostatic loading (see, e.g., [25]). For the fiber-reinforced materials of interest in this work, the appropriate set $\mathcal{K}^{*}$ will be dictated by the construction process described in Sect. 3.2 and 3.3 below. From its definition, it is plain that $\overline{W}^{*} = \overline{W}$ from $\overline{\mathbf{F}} = \mathbf{I}$ all the way up to the onset of a first instability, after which $\overline{W}^{*} \geq \overline{W}$. For notational simplicity, we will drop the use of the symbol $*$ in $\overline{W}^{*}$ henceforth, with the understanding that $\overline{W}$ will denote the effective stored-energy function defined in (7).

[1] In the limiting case of rigid fibers, the range of validity of the linearly elastic solution may vanish for some deformation modes.

[2] This is a rigorous result (see Sect. 5) provided that the local energy $W(\mathbf{X},\mathbf{F}(\mathbf{X}))$ be strictly rank-one convex at all material points $\mathbf{X}$ in the specimen and satisfy some additional technical requirements [20].

3 Iterated dilute homogenization of fiber-reinforced solids in finite elasticity

The main objective of this work is to derive a constitutive theory for fiber-reinforced hyperelastic solids by constructing *exact* solutions of (7) that depend on the prescribed one- and two-point microstructural statistics. To this end, we employ a strategy that comprises two main steps. The first step, described in Sect. 3.1, consists of an iterated homogenization procedure (or differential scheme) in finite elasticity that provides an exact solution for $\overline{W}$ in terms of an auxiliary dilute problem. The second step, described in Sect. 3.2, is concerned with the auxiliary dilute problem, which consists in the construction of a class of fibrous microgeometries whose *matrix* phase is present in dilute concentrations in such a way that their effective stored-energy function can be determined exactly and explicitly up to a set of nonlinear algebraic equations. The combination of these two steps, as carried out in Sect. 3.3, generates an exact stored-energy function $\overline{W}$, given by (33), for a fairly general class of fibrous microgeometries.

3.1 A differential scheme

Differential schemes are iterative processes that make use of results for the effective properties of *dilute* composites in order to generate corresponding results for composites with *finite* phase concentrations. This technique was originally put forward during the 1930s in the context of electrostatics [26], and ever since has repeatedly proved extremely helpful in deriving the macroscopic properties of *linear* composites with a wide range of random microstructures; see, e.g., [27, Chap 10.7] and references therein. By contrast, its use for *nonlinear* composites has not been pursued to nearly the same extent, presumably because of the inherent technical difficulties. Nevertheless, the central idea of this technique is geometrical in nature and can therefore be applied to any constitutively nonlinear problem of choice; see, e.g., [15,28] for applications to small-strain nonlinear elasticity.

In the context of finite elasticity, Lopez-Pamies [29] has recently proposed a differential scheme. The starting point is to consider a class of material systems made up of two constituent phases, characterized by stored-energy functions $W^{(1)}$ and $W^{(2)}$, with geometrically similar microgeometries that are parameterized by the concentration of one of the constituent phases. Let, for instance, that phase be $r = 1$ and denote by $f^{[1]}$ its concentration in this first iteration; throughout this subsection, phase concentrations refer to the undeformed configuration, and a superscript $[k]$ is used to denote quantities associated with the kth iteration in the differential scheme. Now, within that class of microgeometries, consider a sequence of members with decreasing $f^{[1]}$, and assume that the effective stored-energy function $\overline{W}^{[1]}$ associated with those microgeometries exhibits a regular asymptotic behavior as $f^{[1]} \to 0$. We can thus write

$$\overline{W}^{[1]}(\overline{\mathbf{F}}) = W^{(2)}(\overline{\mathbf{F}}) - \mathcal{H}\left[W^{(1)}, W^{(2)}; \overline{\mathbf{F}}\right] f^{[1]} + O(f^{[1]^2}), \tag{8}$$

where $\mathcal{H}$ is a functional[3] with respect to its first two arguments, $W^{(1)}$ and $W^{(2)}$, and a function with respect to its third argument $\overline{\mathbf{F}}$. The specific form of $\mathcal{H}$ depends, of course, on the class of microgeometries being considered. Note, however, that the specific role of the "dilute" phase (e.g., matrix or inclusion phase) is at this stage immaterial.

Next, consider the *same* class of two-phase microgeometries, where the "dilute" phase is again phase 1, but the "non-dilute" phase is characterized by the stored-energy function (8), rather than by $W^{(2)}$. Denote the concentration of phase 1 in this second iteration by $f^{[2]}$, and, again, consider a sequence of microgeometries with decreasing $f^{[2]}$. The effective stored-energy function associated with those microgeometries is, to first order in $f^{[2]}$,

$$\overline{W}^{[2]}(\overline{\mathbf{F}}) = \overline{W}^{[1]}(\overline{\mathbf{F}}) - \mathcal{H}\left[W^{(1)}, \overline{W}^{[1]}; \overline{\mathbf{F}}\right] f^{[2]}, \tag{9}$$

where $\mathcal{H}$ is the *same* functional as in (8). Note that the *total* volume fraction of phase 1 in this two-phase material is now $f^{[2]} + f^{[1]}(1 - f^{[2]})$. Thus, an amount $f^{[2]}(1 - f^{[1]})$ of phase 1 has been added to the material in this second iteration.

[3] That is, $\mathcal{H}$ is an operator (e.g., a differential operator) with respect to the stored-energy functions $W^{(r)}$, so that it can depend, for instance, not just on $W^{(r)}$ but also on any derivative $\partial^n W^{(r)}/\partial \mathbf{F}^n$ $n \in \mathbb{N}$.

It is apparent now that repeating the same above process $k+1$ times, where k is an arbitrarily large integer, generates a two-phase material with effective stored-energy function

$$\overline{W}^{[k+1]}(\overline{\mathbf{F}}) = \overline{W}^{[k]}(\overline{\mathbf{F}}) - \mathcal{H}\left[W^{(1)}, \overline{W}^{[k]}; \overline{\mathbf{F}}\right] f^{[k+1]}, \tag{10}$$

which contains a *total* volume fraction of phase 1 given by

$$c^{[k+1]} = 1 - \prod_{j=1}^{k+1}(1 - f^{[j]}). \tag{11}$$

Furthermore, note that the *increment* in total concentration of the phase 1 in this iteration (i.e., in passing from k to $k+1$) reads as

$$c^{[k+1]} - c^{[k]} = \prod_{j=1}^{k}(1 - f^{[j]}) - \prod_{j=1}^{k+1}(1 - f^{[j]}) = f^{[k+1]}\,(1 - c^{[k]}), \tag{12}$$

from which it is a trivial matter to establish the following identity

$$f^{[k+1]} = \frac{c^{[k+1]} - c^{[k]}}{1 - c^{[k]}}. \tag{13}$$

Next, after substituting (13) in expression (10), we obtain

$$\left(1 - c^{[k]}\right) \frac{\overline{W}^{[k+1]}(\overline{\mathbf{F}}) - \overline{W}^{[k]}(\overline{\mathbf{F}})}{c^{[k+1]} - c^{[k]}} + \mathcal{H}\left[W^{(1)}, \overline{W}^{[k]}; \overline{\mathbf{F}}\right] = 0. \tag{14}$$

This difference equation can be finally recast, upon using the facts that the increment $c^{[k+1]} - c^{[k]}$ is infinitesimally small and that k is arbitrarily large, as the following *initial-value problem*

$$(1 - c_0^{(1)}) \frac{\partial \overline{W}}{\partial c_0^{(1)}} + \mathcal{H}\left[W^{(1)}, \overline{W}; \overline{\mathbf{F}}\right] = 0, \quad \overline{W}(\overline{\mathbf{F}}, 0) = W^{(2)}(\overline{\mathbf{F}}), \tag{15}$$

for the effective stored-energy function $\overline{W}(\overline{\mathbf{F}}, c_0^{(1)})$, where $c_0^{(1)}$ denotes the total concentration of phase 1 in the final microgeometry. Alternatively, the stored-energy function $\overline{W}$ can rewritten as a function of $c_0^{(2)} = 1 - c_0^{(1)}$. The resulting equation for $\overline{W}(\overline{\mathbf{F}}, c_0^{(2)})$ is then given by

$$c_0^{(2)} \frac{\partial \overline{W}}{\partial c_0^{(2)}} - \mathcal{H}\left[W^{(1)}, \overline{W}; \overline{\mathbf{F}}\right] = 0, \quad \overline{W}(\overline{\mathbf{F}}, 1) = W^{(2)}(\overline{\mathbf{F}}). \tag{16}$$

In summary, starting from the effective stored-energy function of any *dilute* microgeometry of choice, as determined by the functional $\mathcal{H}$, the above differential scheme yields an *exact* formulation (in the form of an initial-value problem) for the effective stored-energy function $\overline{W}$ of a material with *finite* values of phase concentrations. For later reference, it is noted that if the dilute microgeometry is of particulate type, the above scheme generates non-dilute microgeometries that are also particulate. This follows from the fact that the same functional $\mathcal{H}$ and the same dilute phase are used at each iteration step.

The usefulness of the exact formulation (16) then hinges upon being able to compute the functional $\mathcal{H}$ describing the relevant dilute response of the composite of interest. In general, it is *not* possible to solve dilute problems in *finite elasticity* by analytical means—this is in contrast to dilute problems in *linear* elasticity for which there is, for instance, the explicit solution of Eshelby [30] and its generalizations. As detailed in the sequel, there is, however, a class of particulate microstructures for which the dilute response functional $\mathcal{H}$ can be computed *exactly*[4] and *explicitly*: sequential laminates [15] (see also [16]).

[4] Alternatively, an analytical solution for $\mathcal{H}$ may be also obtained *approximately* by means of linear comparison methods [31]; this latter approach has already proved fruitful in the related context of dilute distributions of vacuous imperfections and cavitation instabilities [32].

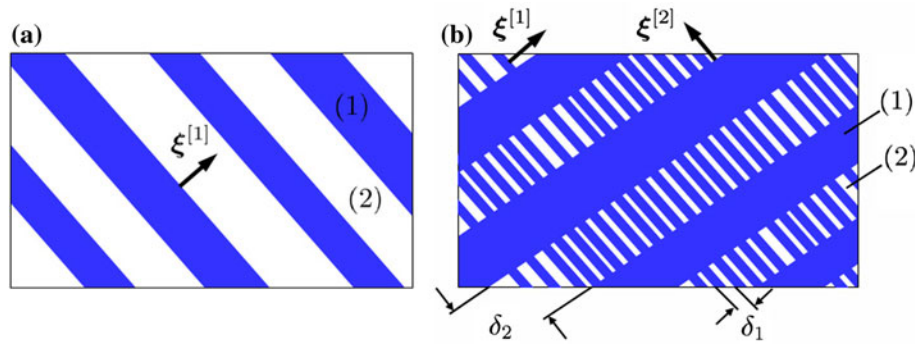

Fig. 1 Sequential laminates in their undeformed configurations: **a** simple or rank 1 laminate with lamination direction $\boldsymbol{\xi}^{[1]}$, **b** rank 2 laminate with lamination direction $\boldsymbol{\xi}^{[2]} (\delta_2 \gg \delta_1)$

3.2 The "dilute" microgeometries: sequential laminates

A sequential laminate is an iterative construction obtained by layering laminated materials (which in turn have been obtained from lower-order lamination procedures) with other laminated materials, or directly with the homogeneous phases that make up the composite, in such a way as to produce hierarchical microgeometries of increasing complexity; see, e.g., [27, Chap. 9]. The *rank* of the laminate refers to the number of layering operations required to reach the final sequential laminate. Below, we follow a strategy similar to that put forward by Idiart [15] in the context of small-strain nonlinear elasticity to compute the effective stored-energy function of a general class of hyperelastic sequential laminates.

The starting point in constructing sequential laminates is to consider a simple, or rank-1, laminate with a given layering direction $\boldsymbol{\xi}^{[1]}$, and with phases 1 and 2 in proportions $(1 - f^{[1]})$ and $f^{[1]}$, respectively, as shown in Fig. 1a; throughout this subsection, layering directions and concentrations refer to the undeformed configuration, and a superscript $[i]$ is used to mark quantities associated with a rank-i laminate.[5] The characteristic functions $\chi_0^{(r)}$ describing this rank-1 laminated microgeometry depend on $\mathbf{X}$ only through the combination $\mathbf{X} \cdot \boldsymbol{\xi}^{[1]}$. It then follows that the Euler–Lagrange equations associated with (5) admit solutions consisting of *uniform-per-layer* deformation gradient fields. Thus, restricting the set of admissible fields to uniform-per-layer deformations, and denoting the uniform deformation gradient in phase r by $\mathbf{F}^{(r)}$, we observe that continuity of the displacement field and boundary conditions require that

$$\mathbf{F}^{(1)} - \mathbf{F}^{(2)} = \boldsymbol{\omega}^{[1]} \otimes \boldsymbol{\xi}^{[1]}, \tag{17}$$

$$(1 - f^{[1]})\, \mathbf{F}^{(1)} + f^{[1]}\, \mathbf{F}^{(2)} = \overline{\mathbf{F}}, \tag{18}$$

for some arbitrary vector $\boldsymbol{\omega}^{[1]}$. Solving for the fields $\mathbf{F}^{(r)}$, we obtain

$$\mathbf{F}^{(1)} = \overline{\mathbf{F}} + f^{[1]}\, \boldsymbol{\omega}^{[1]} \otimes \boldsymbol{\xi}^{[1]}, \tag{19}$$

$$\mathbf{F}^{(2)} = \overline{\mathbf{F}} - (1 - f^{[1]})\, \boldsymbol{\omega}^{[1]} \otimes \boldsymbol{\xi}^{[1]}, \tag{20}$$

so that the effective stored-energy function of the rank-1 laminate can be written as (see, e.g., [16])

$$\overline{W}^{[1]}(\overline{\mathbf{F}}) = \min_{\boldsymbol{\omega}^{[1]}} \left\{ (1 - f^{[1]}) W^{(1)} \left(\mathbf{F}^{(1)} \right) + f^{[1]}\, W^{(2)} \left(\mathbf{F}^{(2)} \right) \right\}. \tag{21}$$

The optimality condition with respect to $\boldsymbol{\omega}^{[1]}$ implies continuity of the traction vector across material interfaces in the undeformed configuration. Given that the set of kinematically admissible fields has been restricted to uniform-per-layer fields, we see that expression (21) corresponds to the unique exact effective stored-energy function up to the onset of the first instability. Beyond that point along a deformation path, other solutions that are not uniform per layer exist (see, e.g., [33,34]) that may correspond to lower overall energies, as already discussed in Sect. 2.

[5] The use of similar notation to that of Sect. 3.1 should not lead to confusion.

Sequential laminates are now constructed by an iterative process. Of all possible types of two-phase sequential laminates, we restrict attention to laminates formed by layering at every step a laminate with one of the original phases, say $r = 1$; as will be seen below, this phase will play the role of the matrix. A rank-2 laminate is thus constructed by layering the above rank-1 laminate with phase $r = 1$, in proportions $f^{[2]}$ and $1 - f^{[2]}$, respectively, along a certain layering direction $\boldsymbol{\xi}^{[2]}$, as shown schematically in Fig. 1b. The key assumption in this construction process is that the length scale of the *embedded* laminate is taken to be much smaller than the length scale of the *embedding* laminate, i.e., $\delta_1 << \delta_2$ in Fig. 1b, so that in the rank-2 laminate, the rank-1 laminate can be regarded as a homogeneous phase. Consequently, the effective stored-energy function $\overline{W}^{[2]}$ of the rank-2 laminate is given by an expression analogous to (21), with $W^{(2)}$ replaced by $\overline{W}^{[1]}$. The total concentration of phase 2 in the rank-2 laminate is $f^{[1]} f^{[2]}$.

A rank-M laminate is obtained by repeating this process M times, always laminating a rank-m laminate with phase $r = 1$, in proportions $f^{[m]}$ and $(1 - f^{[m]})$, respectively, along a layering direction $\boldsymbol{\xi}^{[m]}$. Making repeated use of the formula (21) for simple laminates, and after some algebraic manipulations, we can easily show that the effective stored-energy function $\overline{W}^{[M]}$ of the rank-M laminate is given by [15]

$$\overline{W}^{[M]}(\overline{\mathbf{F}}) = \min_{\substack{\boldsymbol{\omega}^{[i]} \\ i=1,\ldots,M}} \left\{ c_0^{(2)}\, W^{(2)}\left(\overline{\mathbf{F}}^{(2)}\right) + \sum_{i=1}^{M} (1 - f^{[i]}) \prod_{j=i+1}^{M} f^{[j]} W^{(1)}\left(\mathbf{F}^{[i]}\right) \right\}, \tag{22}$$

where $c_0^{(2)} = \prod_{i=1}^{M} f^{[i]}$ is the total volume fraction of phase 2, and the deformation gradient tensors $\mathbf{F}^{[i]}$ and $\overline{\mathbf{F}}^{(2)}$ are given by

$$\mathbf{F}^{[i]} = \overline{\mathbf{F}} + f^{[i]}\, \boldsymbol{\omega}^{[i]} \otimes \boldsymbol{\xi}^{[i]} - \sum_{j=i+1}^{M} (1 - f^{[j]})\, \boldsymbol{\omega}^{[j]} \otimes \boldsymbol{\xi}^{[j]}, \quad i = 1, \ldots, M, \tag{23}$$

$$\overline{\mathbf{F}}^{(2)} = \overline{\mathbf{F}} - \sum_{i=1}^{M} (1 - f^{[i]})\, \boldsymbol{\omega}^{[i]} \otimes \boldsymbol{\xi}^{[i]}. \tag{24}$$

An equivalent formula for $\overline{W}$ was derived by deBotton [16] in recursive form.

Once again, note that each iteration step in the above construction process makes use of a set of kinematically admissible fields that is restricted to uniform-per-layer deformation gradients. From their construction process, it follows that these sequentially laminated microgeometries can be regarded as *random* and *particulate*, with phase 2 playing the role of the inclusion (discontinuous) phase, surrounded by a (continuous) matrix made up of phase 1; see Fig. 1. A peculiar feature of these microgeometries, of particular importance in the following, is that the deformation gradient field within the *fiber* phase is *uniform*. This follows immediately from the fact that the stored-energy function $W^{(2)}$ characterizing the fiber phase appears in expression (22) evaluated at a single value of deformation given by (24). Within the matrix phase, by contrast, the deformation gradient field is non-uniform, taking on M different values given by (23).

The symmetry of sequentially laminated microgeometries increases with increasing rank. In fact, extreme degrees of symmetry such as transverse isotropy, which are of particular interest here, can only be achieved in the limit of infinite rank. As noted by deBotton [16], taking the limit $M \to \infty$ directly in expression (22) is not straightforward due to the fact that $\overline{W}^{[M]}$ depends on the order of the lamination sequence $\{(f^{[1]}, \boldsymbol{\xi}^{[1]}), \ldots, (f^{[M]}, \boldsymbol{\xi}^{[M]})\}$. When the matrix phase is present in dilute concentrations, however, such a dependence disappears and the limit can be easily evaluated as shown next.

Motivated by the work of deBotton [16], we consider "dilute" rank-M laminates characterized by volume fractions of the form

$$f^{[i]} = 1 - \nu^{[i]} c_0^{(1)}, \quad \text{with } \nu^{[i]} \geq 0, \quad \sum_{i=1}^{M} \nu^{[i]} = 1, \tag{25}$$

where $c_0^{(1)}$ is an *infinitesimally small* quantity. The constraint $(25)_3$ is such that the total volume fraction of the *matrix* phase in the undeformed configuration is precisely $c_0^{(1)}$, to first order. Because the interest here is to model fiber-reinforced solids, we restrict attention to rank-M laminates exhibiting *cylindrical* symmetry. Thus, the M layering directions $\boldsymbol{\xi}^{[i]}$ are all taken to lie on a single plane whose normal is identified with the orientation of the fibers $\mathbf{N}$. Furthermore, we take $\boldsymbol{\xi}^{[i]} \neq \boldsymbol{\xi}^{[j]}$ for all $i \neq j$. A particular member in this class of microgeometries is thus specified by a set of constants $\nu^{[i]}$ and unit vectors $\boldsymbol{\xi}^{[i]}$. Assuming that the expansion of the optimal $\boldsymbol{\omega}^{[i]}$ for small $c_0^{(1)}$ is regular, and expanding terms inside the curly brackets in (22) about $c_0^{(1)} = 0$, we obtain the following expression for the effective stored-energy function to first order in $c_0^{(1)}$:

$$\overline{W}^{[M]}(\overline{\mathbf{F}}) = \min_{\substack{\boldsymbol{\omega}^{[i]} \\ i=1,\ldots,M}} \left\{ (1-c_0^{(1)}) W^{(2)}(\overline{\mathbf{F}}) - c_0^{(1)} \sum_{i=1}^{M} \nu^{[i]} \left[\boldsymbol{\omega}^{[i]} \cdot \frac{\partial W^{(2)}}{\partial \overline{\mathbf{F}}}(\overline{\mathbf{F}}) \boldsymbol{\xi}^{[i]} - W^{(1)} \left(\overline{\mathbf{F}} + \boldsymbol{\omega}^{[i]} \otimes \boldsymbol{\xi}^{[i]} \right) \right] \right\}. \quad (26)$$

It can be seen that the contributions to $\overline{W}^{[M]}$ from each lamination i are decoupled.[6] It is now convenient to introduce the generalized function

$$\nu(\boldsymbol{\xi}) = \sum_{i=1}^{M} \nu^{[i]} \, \delta(\boldsymbol{\xi} - \boldsymbol{\xi}^{[i]}) \quad (27)$$

defined over the set of unit vectors $\boldsymbol{\xi}$ that are orthogonal to the fiber direction $\mathbf{N}$; $\delta(\boldsymbol{\xi})$ denotes the Dirac delta function. Expression (26) can then be rewritten as

$$\overline{W}(\overline{\mathbf{F}}) = \min_{\boldsymbol{\omega}(\boldsymbol{\xi})} \left\{ (1-c_0^{(1)}) W^{(2)}(\overline{\mathbf{F}}) - c_0^{(1)} \int_{|\boldsymbol{\xi}|=1} \left[\boldsymbol{\omega} \cdot \frac{\partial W^{(2)}}{\partial \mathbf{F}}(\overline{\mathbf{F}}) \boldsymbol{\xi} - W^{(1)} \left(\overline{\mathbf{F}} + \boldsymbol{\omega} \otimes \boldsymbol{\xi} \right) \right] \nu(\boldsymbol{\xi}) \mathrm{d}\boldsymbol{\xi} \right\}, \quad (28)$$

where the minimization operation is now over vector functions $\boldsymbol{\omega}(\boldsymbol{\xi})$ defined over the set of unit vectors $\boldsymbol{\xi}$, and the superscript $[M]$ has been dropped to ease notation. This expression is valid for laminates of *finite* as well as *infinite* rank: in the first case, the function $\nu(\boldsymbol{\xi})$ is a sum of Dirac masses, while in the second case, it is a continuous function of $\boldsymbol{\xi}$. In view of the constraint $(25)_3$, the function $\nu(\boldsymbol{\xi})$ always satisfies the constraint

$$\int_{|\boldsymbol{\xi}|=1} \nu(\boldsymbol{\xi}) \mathrm{d}\boldsymbol{\xi} = 1, \quad (29)$$

so that the operation

$$\langle \cdot \rangle \equiv \int_{|\boldsymbol{\xi}|=1} (\cdot) \nu(\boldsymbol{\xi}) \mathrm{d}\boldsymbol{\xi} \quad (30)$$

corresponds to a weighted orientational average on the transverse plane. The result (28) can thus be written as

$$\overline{W}(\overline{\mathbf{F}}) = W^{(2)}(\overline{\mathbf{F}}) - \left[W^{(2)}(\overline{\mathbf{F}}) + \max_{\boldsymbol{\omega}(\boldsymbol{\xi})} \left\langle \boldsymbol{\omega} \cdot \frac{\partial W^{(2)}}{\partial \mathbf{F}}(\overline{\mathbf{F}}) \boldsymbol{\xi} - W^{(1)} \left(\overline{\mathbf{F}} + \boldsymbol{\omega} \otimes \boldsymbol{\xi} \right) \right\rangle \right] c_0^{(1)}. \quad (31)$$

This expression constitutes an exact result for the effective stored-energy function of a class of *infinite*-rank laminates with *infinitesimal matrix* concentrations.

It is emphasized that phase 2 plays the role of cylindrical fibers that are aligned with $\mathbf{N}$ and surrounded by a continuous matrix made up of phase 1; see Fig. 1. The function $\nu(\boldsymbol{\xi})$ characterizes the in-plane distribution of fibers,

[6] Bourdin and Kohn [35] have shown in the context of linear elasticity that, to first order in $c_0^{(1)}$, these sequential laminates can be regarded as intersecting families of parallel walls, which act independently of each other so that the effective behavior is given by the sum of their individual behavior, weighted by the relative concentrations $\nu^{[i]}$.

and will be related to the two-point microstructural statistics below. Finally, we note that the optimality condition in (31) is given by

$$\left[\frac{\partial W^{(2)}}{\partial \mathbf{F}}(\overline{\mathbf{F}}) - \frac{\partial W^{(1)}}{\partial \mathbf{F}}\left(\overline{\mathbf{F}} + \boldsymbol{\omega}\otimes\boldsymbol{\xi}\right)\right]\boldsymbol{\xi} = \mathbf{0}, \tag{32}$$

which is a nonlinear algebraic equation for $\boldsymbol{\omega}$ (at a given $\boldsymbol{\xi}$), and states continuity of the traction vector across material interfaces in the undeformed configuration, as expected.

3.3 The iterated dilute homogenization model

We are now in a position to formulate a constitutive model for fiber-reinforced solids. Indeed, focusing first on expression (31), it is observed that the effective stored-energy function for the "dilute" microgeometries constructed in Sect. 3.2 is of the regular form assumed in the differential scheme of Sect. 3.1 (namely, linear in $c_0^{(1)}$), with the functional $\mathcal{H}$ given by the square brackets in (31). Then, by making use of (31) in (16), it is a simple matter to deduce that the effective stored-energy function $\overline{W}(\overline{\mathbf{F}}, c_0)$ for the above-constructed class of fiber-reinforced hyperelastic solids is solution of the following nonlinear first-order partial differential equation:

$$c_0\frac{\partial \overline{W}}{\partial c_0} - H\left(\overline{\mathbf{F}}, \overline{W}, \frac{\partial \overline{W}}{\partial \overline{\mathbf{F}}}\right) = 0, \quad \overline{W}(\overline{\mathbf{F}}, 1) = W^{(2)}(\overline{\mathbf{F}}), \tag{33}$$

where $c_0 \equiv c_0^{(2)}$ denotes the concentration of fibers in the undeformed configuration, and

$$H\left(\overline{\mathbf{F}}, \overline{W}, \overline{\mathbf{S}}\right) = \overline{W} + \max_{\boldsymbol{\omega}(\boldsymbol{\xi})}\left\langle \boldsymbol{\omega}\cdot\overline{\mathbf{S}}\boldsymbol{\xi} - W^{(1)}\left(\overline{\mathbf{F}} + \boldsymbol{\omega}\otimes\boldsymbol{\xi}\right)\right\rangle. \tag{34}$$

Here, it is important to emphasize that the exact result (33) is general enough to allow for any matrix and fiber stored-energy functions ($W^{(1)}$ and $W^{(2)}$) and completely general loading conditions ($\overline{\mathbf{F}}$). In addition, it allows for fairly general in-plane fiber distributions, as characterized by the orientational average (30). A class of distributions which is particularly important in applications and allows explicit evaluation of $\nu(\boldsymbol{\xi})$ in the orientational average (30) is that of "elliptical" distributions, introduced by Willis [36]. This is a generalization of isotropic distributions, and postulates that the two-point probabilities (3) exhibit elliptical symmetry. More precisely, it is postulated that

$$h(\mathbf{X}) \equiv h(|\mathbf{A}\hat{\mathbf{X}}|), \tag{35}$$

where the second-order tensor $\mathbf{A}$ serves to characterize the "shape" and "orientation" of the assumed in-plane elliptical distribution, such that $\mathbf{A} = \mathbf{I}$ corresponds to statistical isotropy. The associated function $\nu(\boldsymbol{\xi})$ can be shown [15] to be

$$\nu(\boldsymbol{\xi}) = \frac{1}{2\pi\,\det\mathbf{A}}|\mathbf{A}\boldsymbol{\xi}|^{-1}, \tag{36}$$

which is seen to depend on the "angular" variation of the two-point probability $\hat{h}$, but *not* on its "radial" variation.

It is also important to emphasize that, by construction, the homogenization result (33) is *realizable*, in the sense that it is exact for a given class of microgeometries. Consequently, the effective stored-energy function $\overline{W}$ is guaranteed to be theoretically sound and to give physically sensible predictions. In particular, $\overline{W}$ is guaranteed to be objective in $\overline{\mathbf{F}}$, to satisfy all pertinent bounds, to linearize properly, and to comply with any macroscopic constraints imposed by microscopic constraints, such as the strongly nonlinear constraint of incompressibility $\det\overline{\mathbf{F}} = 1$.

From a mathematical point of view, it is interesting to note that the nonlinear first-order partial differential equation (33) corresponds to a Hamilton–Jacobi equation where the fiber concentration c_0 and the macroscopic deformation gradient $\overline{\mathbf{F}}$ play the role of "time" and "space" variables, respectively, and the function H plays the role of a Hamiltonian; see, e.g., [37, Chap. 14]. In this regard, note that the matrix behavior, fiber orientation $\mathbf{N}$, and in-plane fiber distribution function $\nu(\boldsymbol{\xi})$ are contained in the Hamiltonian (34), while the fiber behavior dictates the "initial" condition.

In view of its generality and realizability, we propose the effective stored-energy function $\overline{W}$ defined by (33) as a constitutive model for the macroscopic response of fiber-reinforced hyperelastic solids. The inputs for this model are the properties of the matrix and fibers, as characterized by their stored-energy functions $W^{(1)}$ and $W^{(2)}$, and the one- and two-point statistics of the microstructure, as characterized by the volume fraction of fibers c_0 and the orientational average $\langle\cdot\rangle$, which contain information about the size, shape, and orientation of the fibers.

3.3.1 Infinitesimal deformations

In the limit of small deformations as $\overline{\mathbf{F}} \to \mathbf{I}$, Eq. 33 can be solved explicitly. Indeed, the solution for $\overline{W}$ in this case must be of the asymptotic form

$$\overline{W}(\overline{\mathbf{F}}, c_0) = \frac{1}{2}\overline{\boldsymbol{\varepsilon}} \cdot \widetilde{\boldsymbol{\mathcal{L}}}_0 \overline{\boldsymbol{\varepsilon}} + O\left(||\overline{\mathbf{F}} - \mathbf{I}||^3\right), \tag{37}$$

where $\overline{\boldsymbol{\varepsilon}} = (\overline{\mathbf{F}} + \overline{\mathbf{F}}^T - 2\mathbf{I})/2$ is the macroscopic infinitesimal strain tensor, and $\widetilde{\boldsymbol{\mathcal{L}}}_0$ is an effective fourth-order modulus tensor that depends on the microstructure and on the local moduli $\boldsymbol{\mathcal{L}}_0^{(r)}$, but not on $\overline{\boldsymbol{\varepsilon}}$. An equation for $\widetilde{\boldsymbol{\mathcal{L}}}_0$ follows from expanding the Hamilton–Jacobi equation (33) about $\overline{\mathbf{F}} = \mathbf{I}$. The relevant Hamiltonian (34) is derived in Appendix A, [see expression (100)], and the resulting equation for $\widetilde{\boldsymbol{\mathcal{L}}}_0$ can be shown to reduce simply to

$$c_0 \frac{\partial \widetilde{\boldsymbol{\mathcal{L}}}_0}{\partial c_0} - \Delta\widetilde{\boldsymbol{\mathcal{L}}}_0 - \Delta\widetilde{\boldsymbol{\mathcal{L}}}_0 \boldsymbol{\mathcal{P}} \Delta\widetilde{\boldsymbol{\mathcal{L}}}_0 = 0, \quad \widetilde{\boldsymbol{\mathcal{L}}}_0\big|_{c_0=1} = \boldsymbol{\mathcal{L}}_0^{(2)}, \tag{38}$$

where $\Delta\widetilde{\boldsymbol{\mathcal{L}}}_0 \equiv \widetilde{\boldsymbol{\mathcal{L}}}_0 - \boldsymbol{\mathcal{L}}_0^{(1)}$. The solution to this equation is given by

$$\widetilde{\boldsymbol{\mathcal{L}}}_0 = \boldsymbol{\mathcal{L}}_0^{(1)} + c_0 \left[(1-c_0)\boldsymbol{\mathcal{P}} + (\boldsymbol{\mathcal{L}}_0^{(2)} - \boldsymbol{\mathcal{L}}_0^{(1)})^{-1}\right]^{-1}, \tag{39}$$

where $\boldsymbol{\mathcal{P}}$ is a microstructural tensor that depends on the function $\nu(\boldsymbol{\xi})$; see expression (101) in Appendix A.

For "elliptical" microstructures with $\nu(\boldsymbol{\xi})$ given by (36), expression (39) agrees *exactly* with the linear Willis estimate [36], which is known to be reasonably accurate for fiber-reinforced materials with aligned cylindrical fibers of elliptical cross-section, at least for small to moderate fiber concentrations [38]. Moreover, in the limit of small concentration of fibers ($c_0 \to 0$), the result (39) recovers the exact solution of Eshelby [30] for the problem of a fiber of elliptical cross-section embedded in an infinite matrix. These connections indicate that the nonlinear estimate (33) should indeed be appropriate to model fiber-reinforced solids with particulate microstructures. It is also worth remarking that if the constituent phases are well-ordered, i.e., $(\boldsymbol{\mathcal{L}}_0^{(2)} - \boldsymbol{\mathcal{L}}_0^{(1)})$ is a positive-definite tensor, the estimate (39) attains the Hashin–Shtrikman *lower* bound for the effective moduli of fiber-reinforced materials. Finally, it is interesting to remark that McLaughlin [39] arrived at the same Eq. 38 by making use a differential scheme and the exact solution for a dilute distribution of fibers, as opposed to a dilute distribution of matrix, in a linearly elastic infinite medium.

3.3.2 Incompressible constituents

In the case of incompressible matrix constituents (i.e., $W^{(1)}(\mathbf{F}) = +\infty$ if $\det \mathbf{F} \neq 1$), the Hamiltonian H simplifies considerably. Indeed, if the *matrix* phase is incompressible, the argument of $W^{(1)}$ in (34) must have determinant equal to one. Now,

$$\det\left(\overline{\mathbf{F}} + \boldsymbol{\omega} \otimes \boldsymbol{\xi}\right) = \det \overline{\mathbf{F}} \ \det\left(\mathbf{I} + \overline{\mathbf{F}}^{-1}\boldsymbol{\omega} \otimes \boldsymbol{\xi}\right) = \overline{J}\left[1 + (\overline{\mathbf{F}}^{-1}\boldsymbol{\omega} \cdot \boldsymbol{\xi})\right], \tag{40}$$

and therefore, the optimal vector $\boldsymbol{\omega}$ must satisfy the constraint

$$\overline{\mathbf{F}}^{-1}\boldsymbol{\omega} \cdot \boldsymbol{\xi} = \frac{1-\overline{J}}{\overline{J}}, \tag{41}$$

where $\overline{J} \equiv \det \overline{\mathbf{F}}$. Thus, the optimal vector $\boldsymbol{\omega}$ must be of the form

$$\boldsymbol{\omega} = \frac{1-\overline{J}}{\overline{J}}\overline{\mathbf{F}}\boldsymbol{\xi} + \omega_\perp \overline{\mathbf{F}}\boldsymbol{\xi}^\perp + \omega_N \overline{\mathbf{F}}\mathbf{N}, \tag{42}$$

where $\boldsymbol{\xi}^{\perp}$ is a unit vector orthogonal to $\boldsymbol{\xi}$ and $\mathbf{N}$, and the components $\omega_{\perp}$ and ω_N are functions of $\boldsymbol{\xi}$. The three-dimensional optimization in the Hamiltonian (34) is thus reduced to a two-dimensional optimization with respect to $\omega_{\perp}$ and ω_N.

If the *fibers* are also incompressible (i.e., $W^{(2)}(\mathbf{F}) = +\infty$ if $\det \mathbf{F} \neq 1$), the fiber-reinforced solid as a whole is macroscopically incompressible. Then, $\overline{J} = 1$ and the vector $\boldsymbol{\omega}$ reduces further to

$$\boldsymbol{\omega} = \omega_{\perp}\overline{\mathbf{F}}\boldsymbol{\xi}^{\perp} + \omega_N\overline{\mathbf{F}}\mathbf{N}. \tag{43}$$

For the special case of plane-strain loading conditions, $\omega_N = 0$ and expression (43) reduces to an earlier result of deBotton [16].

3.3.3 Transversely isotropic materials

When the in-plane fiber distribution is isotropic and the local stored-energy functions $W^{(r)}$ are transversely isotropic functions of $\mathbf{F}$ with symmetry axis $\mathbf{N}$, the macroscopic behavior of the fiber-reinforced material is also transversely isotropic with symmetry axis $\mathbf{N}$. For these material systems, the microstructural function $\nu(\boldsymbol{\xi})$ is given by (36) with $\mathbf{A} = \mathbf{I}$, that is

$$\nu(\boldsymbol{\xi}) = \frac{1}{2\pi}, \tag{44}$$

and the stored-energy functions are of the form

$$W^{(r)}(\mathbf{F}) = \Psi^{(r)}(I_1, I_2, I_3, I_4, I_5), \tag{45}$$

where the I_α's ($\alpha = 1, 2, \ldots, 5$) denote the five transversely isotropic invariants of the right Cauchy–Green deformation tensor $\mathbf{C} = \mathbf{F}^T\mathbf{F}$ about $\mathbf{N}$:

$$I_1 = \mathrm{tr}\mathbf{C}, \quad I_2 = \frac{1}{2}\left[(\mathrm{tr}\mathbf{C})^2 - \mathrm{tr}\mathbf{C}^2\right], \quad I_3 = \det \mathbf{C}, \quad I_4 = \mathbf{N}\cdot\mathbf{C}\mathbf{N}, \quad I_5 = \mathbf{N}\cdot\mathbf{C}^2\mathbf{N}. \tag{46}$$

Likewise, the effective stored-energy function $\overline{W}$ is of the form

$$\overline{W}(\overline{\mathbf{F}}, c_0) = \overline{\Psi}(\overline{I}_1, \overline{I}_2, \overline{I}_3, \overline{I}_4, \overline{I}_5, c_0), \tag{47}$$

where the $\overline{I}_\alpha$'s ($\alpha = 1, 2, \ldots, 5$) denote the five transversely isotropic invariants of $\overline{\mathbf{C}} = \overline{\mathbf{F}}^T\overline{\mathbf{F}}$. Thus, the Hamilton–Jacobi equation (33) for $\overline{\Psi}$ can be formally simplified (with a slight abuse of notation) to

$$c_0\frac{\partial\overline{\Psi}}{\partial c_0} - H\left(\overline{I}_\alpha, \overline{\Psi}, \frac{\partial\overline{\Psi}}{\partial\overline{I}_\alpha}\right) = 0 \tag{48}$$

with initial condition $\overline{\Psi}(\overline{I}_1, \overline{I}_2, \overline{I}_3, \overline{I}_4, \overline{I}_5, 1) = \Psi^{(2)}(\overline{I}_1, \overline{I}_2, \overline{I}_3, \overline{I}_4, \overline{I}_5)$. Note that the "space" dimension is thus reduced from nine (i.e., the 9 components $\overline{F}_{ij}$) to five (i.e., the 5 invariants $\overline{I}_\alpha$).

If, in addition, the constituent phases are *incompressible*, the fiber-reinforced solid is macroscopically incompressible, and so $\overline{I}_3 = \overline{J}^2 = 1$. The "space" dimension in (48) thus reduces further, to four. In this context, it is relevant to record that the resulting Hamilton–Jacobi equation admits a closed-form solution for the special case of aligned *axisymmetric* loading so that $\overline{I}_1 = \overline{I}_4 + 2/\sqrt{\overline{I}_4}$, $\overline{I}_2 = 2\sqrt{\overline{I}_4} + 1/\overline{I}_4$, and $\overline{I}_5 = \overline{I}_4^2$. Indeed, it is straightforward to show (see Appendix B) that the Hamilton–Jacobi equation (48) in this case reduces (with a slight abuse of notation) to

$$c_0\frac{\partial\overline{\Psi}}{\partial c_0} - \overline{\Psi} + \Psi^{(1)}(\overline{I}_1, \overline{I}_2, \overline{I}_4, \overline{I}_5) = 0, \quad \overline{\Psi}|_{c_0=1} = \Psi^{(2)}(\overline{I}_1, \overline{I}_2, \overline{I}_4, \overline{I}_5). \tag{49}$$

The solution to this equation is simply given by

$$\overline{\Psi}(\overline{I}_1, \overline{I}_2, \overline{I}_4, \overline{I}_5, c_0) = (1 - c_0)\Psi^{(1)}(\overline{I}_1, \overline{I}_2, \overline{I}_4, \overline{I}_5) + c_0\Psi^{(2)}(\overline{I}_1, \overline{I}_2, \overline{I}_4, \overline{I}_5), \tag{50}$$

which is seen to be nothing more than the arithmetic average of the local stored-energy functions, commonly referred to as the Voigt upper bound [40]. As discussed by He et al. [41], the Voigt upper bound (50), which depends on the microstructure only via the volume fraction of fibers c_0, happens to be an exact solution for the macroscopic response of incompressible transversely isotropic fiber-reinforced solids under aligned *axisymmetric* loading. The proposed *realizable* stored-energy function (48) recovers this exact result, as expected.

3.3.4 Local fields

In addition to the effective stored-energy function $\overline{W}$, a full characterization of the macroscopic response of fiber-reinforced hyperelastic solids may require information on the local fields within the matrix and the fiber phases. For instance, average information on the deformation and stress fields can be used to infer the evolution of the microstructure resulting from the finite changes in geometry, and to detect the onset of some local material instabilities as well as damage, e.g., matrix cavitation or the debonding between matrix and fibers, during the deformation process.

In the context of the present formulation, it can be shown that the local fields within the *fiber* phase are *uniform*, that is, all fibers undergo the same spatially constant deformation and withstand the same spatially constant stress [42]. An equation for the single value of deformation gradient $\overline{\mathbf{F}}^{(2)}$ in the fiber phase can be obtained following a procedure proposed by Idiart and Ponte Castañeda [43] in the context of small-strain elasticity nonlinear. This procedure exploits the identity

$$\overline{\mathbf{F}}^{(2)} = \mathbf{I} + \frac{1}{c_0}\frac{\partial \overline{W}_\tau}{\partial \boldsymbol{\tau}^{(2)}}\bigg|_{\boldsymbol{\tau}^{(2)}=\mathbf{0}}, \tag{51}$$

where $\overline{W}_\tau$ is the effective stored-energy function of a fiber-reinforced solid with perturbed stored-energy function for the fibers of the form

$$W_\tau^{(2)}(\mathbf{F}) = W^{(2)}(\mathbf{F}) + \boldsymbol{\tau}^{(2)} \cdot (\mathbf{F} - \mathbf{I}). \tag{52}$$

The second-order tensor $\boldsymbol{\tau}^{(2)}$ in this expression is a perturbation (material) parameter, such that for $\boldsymbol{\tau}^{(2)} = \mathbf{0}$ the perturbed energy $W_\tau^{(2)}$ reduces to $W^{(2)}$.

Within the constitutive theory proposed here, the function $\overline{W}_\tau$ is solution to the Hamilton–Jacobi equation (33) with initial condition given by (52):

$$c_0\frac{\partial \overline{W}_\tau}{\partial c_0} - H\left(\overline{\mathbf{F}}, \overline{W}_\tau, \frac{\partial \overline{W}_\tau}{\partial \overline{\mathbf{F}}}\right) = 0, \quad \overline{W}_\tau(\overline{\mathbf{F}}, 1) = W_\tau^{(2)}(\overline{\mathbf{F}}), \tag{53}$$

Differentiating this equation throughout with respect to $\boldsymbol{\tau}^{(2)}$ we obtain

$$c_0\frac{\partial}{\partial c_0}\left(\frac{\partial \overline{W}_\tau}{\partial \tau_{ij}^{(2)}}\right) - \frac{\partial \overline{W}_\tau}{\partial \tau_{ij}^{(2)}} - \left\langle \omega_k \frac{\partial}{\partial \overline{F}_{kl}}\left(\frac{\partial \overline{W}_\tau}{\partial \tau_{ij}^{(2)}}\right)\xi_l \right\rangle = 0, \tag{54}$$

where use has been made of the fact that the Hamiltonian is stationary with respect to $\boldsymbol{\omega}$. Making use of the identity (51) in this expression yields the following equation for the tensor function $\overline{\mathbf{F}}^{(2)}(\overline{\mathbf{F}}, c_0)$:

$$c_0\frac{\partial \overline{F}_{ij}^{(2)}}{\partial c_0} - \frac{\partial \overline{F}_{ij}^{(2)}}{\partial \overline{F}_{kl}}\langle \omega_k \xi_l \rangle = 0, \quad \overline{F}_{ij}^{(2)}(\overline{\mathbf{F}}, 1) = \overline{F}_{ij}, \tag{55}$$

where the vector $\boldsymbol{\omega}$ solves the optimality condition in the unpertubed Hamiltonian (34) for $\overline{W}$. This vector $\boldsymbol{\omega}$ is a function of $\overline{\mathbf{F}}$ and c_0, but not of $\overline{\mathbf{F}}^{(2)}$. *Thus, expression (55) constitutes a set of 9 independent linear Hamilton–Jacobi equations for the 9 components of* $\overline{\mathbf{F}}^{(2)}$. It can be shown that even though the perturbed energy (52) is not an objective function of $\mathbf{F}$, the resulting $\overline{\mathbf{F}}^{(2)}$ is an objective function of $\overline{\mathbf{F}}$ [42]. Once $\overline{\mathbf{F}}^{(2)}$ is determined from this equation, the stress level in the fibers can be readily computed by making use of the fiber constitutive relation:

$$\overline{\mathbf{S}}^{(2)} = \frac{\partial W^{(2)}}{\partial \mathbf{F}}(\overline{\mathbf{F}}^{(2)}). \tag{56}$$

By contrast, the spatial distribution of the local fields in the *matrix* phase is non-uniform, and it is therefore of interest to compute not only their average values, or first moments, but also higher-order average information like the second moments. Such information can be similarly obtained by means of the above procedure based on perturbed energies. However, while important in numerous applications, the analysis carried out in the sequel does not make explicit use of this information. Consequently, the derivations of the relevant expressions are omitted here for conciseness, and deferred to a forthcoming publication [42].

4 Microstructure evolution

The above analysis makes use of a Lagrangian description of the kinematics. The evolution of the microstructure resulting from the finite changes in geometry is thus already accounted for in the homogenized stored-energy function $\overline{W}$. However, even if not necessary to determine the effective behavior, it is still of interest to have direct access to variables characterizing the microstructure evolution, as they provide deeper insight into the observed macroscopic behavior. For material systems like the ones considered in this work, the microstructural variables of most interest are the orientation of the fibers, the average in-plane distortion and rotation of the fibers, and the volume fractions of the phases, all of them in the deformed configuration; for a thorough discussion on microstructural variables, the reader is referred to the works of Lopez-Pamies [17] and Lopez-Pamies and Ponte Castañeda [31]. Within the proposed constitutive theory, these variables can all be deduced from the uniform deformation gradient $\overline{\mathbf{F}}^{(2)}$ undergone by the fibers, making use of the following formulae.

4.1 Volume fractions of phases

The *current* volume fraction of each constituent phase in the deformed configuration is given by the expression

$$c^{(r)} = \frac{\int_{\Omega^{(r)}} \mathrm{d}v}{\int_{\Omega} \mathrm{d}v} = \frac{\int_{\Omega_0^{(r)}} \det \mathbf{F} \mathrm{d}V}{\int_{\Omega_0} \det \mathbf{F} \mathrm{d}V} = \frac{\frac{1}{\Omega_0^{(r)}} \int_{\Omega_0^{(r)}} \det \mathbf{F} \mathrm{d}V}{\det \overline{\mathbf{F}}} c_0^{(r)}, \tag{57}$$

where Ω and $\Omega^{(r)}$ denote, respectively, the domains that the specimen and the constituent phase r occupy in the deformed configuration, and the last identity follows from the fact that $\det \mathbf{F}$ is a null-Lagrangian. Since the deformation gradient in the fibers is uniform in the proposed constitutive theory, the volume fraction of fibers in the deformed configuration $c \equiv c^{(2)}$ is consequently given by

$$c = \frac{\det \overline{\mathbf{F}}^{(2)}}{\det \overline{\mathbf{F}}} c_0, \tag{58}$$

which can be readily obtained from knowledge of $\overline{\mathbf{F}}^{(2)}$. If the fibers are incompressible or rigid, this expression reduces to $c = c_0 / \det \overline{\mathbf{F}}$.

4.2 Fiber orientation

The orientation of the fibers in the deformed configuration is particularly important in the analysis of fiber-reinforced solids, since the rotation of the fibers may serve as a dominant geometric softening/stiffening mechanism [24]. It is given in terms of the initial fiber orientation by the direction of the vector $\mathbf{n} = \overline{\mathbf{F}}^{(2)} \mathbf{N}$. An equation for $\mathbf{n}(\overline{\mathbf{F}}, c_0)$ can be readily obtained by multiplying (55) throughout by N_j:

$$c_0 \frac{\partial n_i}{\partial c_0} - \frac{\partial n_i}{\partial \overline{F}_{kl}} \langle \omega_k \xi_l \rangle = 0, \quad n_i(\overline{\mathbf{F}}, 1) = \overline{F}_{ij} N_j. \tag{59}$$

Interestingly, the solution to this equation is simply given by the initial condition[7], namely,

$$\mathbf{n} = \overline{\mathbf{F}}^{(2)} \mathbf{N} = \overline{\mathbf{F}} \mathbf{N}, \tag{60}$$

which is seen to be independent of the behavior of the constituent phases. That is, the orientation of the fibers in the deformed configuration is therefore purely *kinematic* in nature.

[7] Introducing (60) into the differential equation (59), we get

$$c_0 \frac{\partial (\overline{F}_{ij} N_j)}{\partial c_0} - \frac{\partial (\overline{F}_{ij} N_j)}{\partial \overline{F}_{kl}} \langle \omega_k \xi_l \rangle = -\delta_{ik} \delta_{jl} N_j \langle \omega_k \xi_l \rangle = - \langle \omega_i \xi_l N_l \rangle = 0.$$

The last identity follows from the fact that the vectors $\mathbf{N}$ and $\boldsymbol{\xi}$ are orthogonal.

4.3 In-plane fiber distortion and rotation

Since the deformation gradient in the fibers is uniform, the in-plane fiber distortion and rotation during a deformation process can be conveniently characterized by considering the evolution of an ellipse described on the cross-section of a fiber. In the reference configuration, this ellipse can be identified with the set of points $E_0 = \left\{\mathbf{X}|\mathbf{X}\cdot(\mathbf{Z}_0^T\mathbf{Z}_0)\mathbf{X} \leq 1\right\}$, where the symmetric second-order tensor $\mathbf{Z}_0^T\mathbf{Z}_0$ has two in-plane principal values $1/(z_{01})^2$ and $1/(z_{02})^2$, defining an aspect ratio $a_0 = z_{02}/z_{01}$, and a zero out-of-plane principal value. In the deformed configuration, this ellipse evolves—up to a translation—into the set of points $E = \left\{\mathbf{x}|\mathbf{x}\cdot(\mathbf{Z}^T\mathbf{Z})\mathbf{x} \leq 1\right\}$, where

$$\mathbf{Z} = \mathbf{Z}_0(\overline{\mathbf{F}}^{(2)})^{-1}. \tag{61}$$

The symmetric second-order tensor $\mathbf{Z}^T\mathbf{Z}$ has in-plane principal values $1/(z_1)^2$ and $1/(z_2)^2$, defining an aspect ratio $a = z_2/z_1$ in the deformed configuration. In turn, the principal directions of $\mathbf{Z}^T\mathbf{Z}$ define an in-plane orientation of the fibers in the deformed configuration. The evolution of the average shape and in-plane rotation of the fibers can thus be characterized (through the tensor $\mathbf{Z}$) from the knowledge of the deformation gradient tensor $\overline{\mathbf{F}}^{(2)}$ in the fibers, together with the initial shape and in-plane orientation of the fibers in the reference configuration as determined by the tensor $\mathbf{Z}_0$.

5 Onset of instabilities

As anticipated in previous sections, besides characterizing the macroscopic constitutive response, the theory proposed in Sect. 3.3 also provides information about the onset of instabilities in fiber-reinforced hyperelastic solids. The identification of what types of instabilities can be examined and how they can be computed is the subject of this section.

Henceforth, we restrict attention to materials systems with matrix stored-energy functions $W^{(1)}$ that are strongly elliptic (or strictly rank-one convex) for all applied deformations. By contrast, the stored-energy function $W^{(2)}$ that characterizes the behavior of the fibers is taken to be strongly elliptic only for sufficiently small deformations. The motivation behind these constitutive restrictions is based on experimental evidence. Indeed, the matrix phase in a wide range of fiber-reinforced soft solids is isotropic and not prone to admit localized deformations, hence the restriction of strong ellipticity for $W^{(1)}$. On the other hand, because of their fabrication (or growth) process, most classes of fibers are *anisotropic* and therefore prone to lose strong ellipticity at sufficiently large deformations.

5.1 Local fiber instabilities

A type of instability that may occur in the material systems of interest here corresponds to the fibers losing strong ellipticity; this is a *local* material (as opposed to geometrical) instability. By exploiting the fact that the proposed constitutive formulation grants access not only to the macroscopic response but also to the underlying *local* fields (see Sect. 3.3.4), it is possible to compute the macroscopic deformations $\overline{\mathbf{F}}$ at which $W^{(2)}$ loses strong ellipticity locally along any loading path of choice. In this regard, we define the following local coercivity (or stability) constant:

$$\beta(\overline{\mathbf{F}}) = \min_{||\mathbf{u}||=||\mathbf{v}||=1} Q^{(2)}\left(\mathbf{u},\mathbf{v};\overline{\mathbf{F}}\right), \tag{62}$$

where

$$Q^{(2)}\left(\mathbf{u},\mathbf{v};\overline{\mathbf{F}}\right) = \mathcal{L}^{(2)}_{ijkl}(\overline{\mathbf{F}}^{(2)})\,u_j u_l v_i v_k = \overline{F}^{(2)}_{jp}\overline{F}^{(2)}_{lq}\frac{\partial^2 W^{(2)}}{\partial F_{ip}\partial F_{kq}}(\overline{\mathbf{F}}^{(2)})\,u_j u_l v_i v_k \tag{63}$$

with $\mathcal{L}^{(2)}_{ijkl}(\overline{\mathbf{F}}^{(2)}) = \overline{F}^{(2)}_{jp}\overline{F}^{(2)}_{lq}\partial^2 W^{(2)}(\overline{\mathbf{F}}^{(2)})/\partial F_{ip}\partial F_{kq}$ denoting the tangent modulus tensor of the fibers in the *deformed configuration* evaluated at the *uniform* deformation gradient $\overline{\mathbf{F}}^{(2)}$, which is determined by (55) and is

ultimately a function of the macroscopic deformation $\overline{\mathbf{F}}$. Thus, if $\beta(\overline{\mathbf{F}}) > 0$, the fibers are locally strongly elliptic. Whenever $\beta(\overline{\mathbf{F}}) = 0$ at some point along an arbitrary loading path, the fibers lose strong ellipticity. The search for the set of macroscopic deformations $\overline{\mathbf{F}}$ at which $\beta(\overline{\mathbf{F}}) = 0$ is addressed in Sect. 5.3.

5.2 Macroscopic instabilities

In macroscopic deformation regions where the fibers are strongly elliptic (with $\beta(\overline{\mathbf{F}}) > 0$)—and therefore the entire fiber-reinforced solid is *locally* strongly elliptic—the effective stored-energy function $\overline{W}$ defined by (33) may still lose strong ellipticity, signaling the development of macroscopic (or long wavelength) instabilities. The proof of this remarkable result is due to Geymonat et al. [20], who also proved that the onset of such macroscopic instabilities constitutes a rigorous upper bound to the onset of any other type of geometric instability with finite wavelength (commonly referred to as microscopic instabilities).

Here, it is relevant to remark that for the type of fiber-reinforced materials of interest in this work, based on case studies of unidirectional composites [20,33,34], the first instability to be encountered along an arbitrary loading path is expected to be of long wavelength, at least for volume fractions of fibers that are not too small. Accordingly, for materials with *sufficiently large* volume fraction of fibers, the loss of strong ellipticity of the homogenized behavior defined by the Hamilton–Jacobi formulation (33) would be expected to indicate precisely the development of first instabilities. For materials with very *small* volume fractions of fibers, on the other hand, the loss of strong ellipticity of the homogenized response (33) may *not* signal the onset of the first instabilities (something else may happen at an earlier stage of the loading path), but this condition is expected to provide, however, a useful upper bound for them.

In analogy with the local coercivity constant (62), we then define the following macroscopic coercivity constant:

$$B(\overline{\mathbf{F}}) = \min_{||\mathbf{u}||=||\mathbf{v}||=1} \overline{Q}\left(\mathbf{u}, \mathbf{v}; \overline{\mathbf{F}}\right), \tag{64}$$

where

$$\overline{Q}\left(\mathbf{u}, \mathbf{v}; \overline{\mathbf{F}}\right) = \overline{\mathcal{L}}_{ijkl}(\overline{\mathbf{F}})\, u_j u_l v_i v_k = \overline{F}_{jp}\overline{F}_{lq}\frac{\partial^2 \overline{W}(\overline{\mathbf{F}})}{\partial \overline{F}_{ip}\partial \overline{F}_{kq}}\, u_j u_l v_i v_k \tag{65}$$

and $\overline{\mathcal{L}}_{ijkl}(\overline{\mathbf{F}}) = \overline{F}_{jp}\overline{F}_{lq}\partial^2 \overline{W}(\overline{\mathbf{F}})/\partial \overline{F}_{ip}\partial \overline{F}_{kq}$ corresponds to the tangent modulus tensor of the fiber-reinforced solid in the *deformed configuration*. According to (64), the fiber-reinforced solid is macroscopically stable if $B(\overline{\mathbf{F}}) > 0$. Whenever $B(\overline{\mathbf{F}}) = 0$ at some point along an arbitrary loading path, macroscopic strong ellipticity is lost, signaling the possible development of a long wavelength instability.

5.3 Onset-of-failure surface

Because both, the fiber stored-energy function $W^{(2)}$ and the effective stored-energy function $\overline{W}$, linearize properly in the limit of small deformations ($\overline{\mathbf{F}} \to \mathbf{I}$), we have that $\beta(\mathbf{I}) > 0$ and $B(\mathbf{I}) > 0$. However, as the deformation progresses into the finite-deformation regime along an arbitrary loading path with starting point $\overline{\mathbf{F}} = \mathbf{I}$, a point may be reached at which

$$\beta(\overline{\mathbf{F}}_{\rm cr}) = 0 \quad \text{or} \quad B(\overline{\mathbf{F}}_{\rm cr}) = 0 \tag{66}$$

for some critical $\overline{\mathbf{F}}_{\rm cr}$ and pair of critical vectors $\mathbf{u}_{\rm cr}$ and $\mathbf{v}_{\rm cr}$. The set of all such critical values $\overline{\mathbf{F}}_{\rm cr}$ defines a hypersurface $\mathcal{S}$ in $\overline{\mathbf{F}}$-space delimiting stable from unstable regions for the material response. We refer to such a surface as the *onset-of-failure surface*. Moreover, the critical pairs of orthogonal vectors $\mathbf{u}_{\rm cr}$ and $\mathbf{v}_{\rm cr}$ associated with $\overline{\mathbf{F}}_{\rm cr}$, describe the manner in which strong ellipticity is lost. In particular, $\mathbf{u}_{\rm cr}$ denotes the normal vector to surfaces (in the deformed configuration) in which the fiber or the fiber-reinforced solid (depending on whether $\beta(\overline{\mathbf{F}}_{\rm cr}) = 0$ or $B(\overline{\mathbf{F}}_{\rm cr}) = 0$) softens drastically and therefore the deformation is prone to localize. Furthermore, the vector $\mathbf{v}_{\rm cr}$ indicates the direction within such surfaces in which the fiber or the fiber-reinforced solid softens.

In general, the computation of the onset-of-failure surface defined by condition (66) requires a tedious, but straightforward, numerical scanning process. Essentially, at every deformation increment along the loading path of choice, expressions (63) and (65) must be evaluated for all orthogonal unit vectors $\mathbf{u}$ and $\mathbf{v}$ to check whether $Q^{(2)}$ and $\overline{Q}$ remain positive, or, on the contrary, there are values of $\mathbf{u}$ and $\mathbf{v}$ for which either $Q^{(2)}$ or $\overline{Q}$ vanish and consequently condition (66) is satisfied. For certain special forms of the stored-energy functions $W^{(2)}$ and $\overline{W}$, however, it is possible to write down explicit expressions for $\overline{\mathbf{F}}_{\rm cr}$, $\mathbf{u}_{\rm cr}$, and $\mathbf{v}_{\rm cr}$ at which the condition (66) is first satisfied and therefore at which local fiber (if $\beta(\overline{\mathbf{F}}_{\rm cr}) = 0$) or macroscopic (if $B(\overline{\mathbf{F}}_{\rm cr}) = 0$) instabilities ensue. This is indeed the case for the class of *incompressible*, *transversely isotropic* stored-energy functions that will be studied in Sect. 6, where a first application of the theory is presented.

Before proceeding with the specialization of the critical condition (66) to the above-mentioned class of transversely isotropic materials, it is important to record the following remark. In addition to the local failure characterized by $\beta(\overline{\mathbf{F}}_{\rm cr}) = 0$ and the macroscopic failure characterized by $B(\overline{\mathbf{F}}_{\rm cr}) = 0$, there are other phenomena that can result in failure of the fiber-reinforced solid. These include: (i) matrix cavitation and (ii) fiber debonding. Both of these phenomena are local in nature and their study requires consequently knowledge of the local deformation and stress fields in the matrix and the fibers, respectively, which can be conveniently accessed from the proposed formulation (see Sect. 3.3.4). In this work, for brevity, we will restrict the analysis of failure to local fiber instabilities and macroscopic instabilities, as determined by condition (66).

5.4 A class of transversely isotropic separable stored-energy functions

In the next section, we consider an application of the constitutive theory proposed in Sect. 3 in which the local behavior of the fibers and the resulting macroscopic behavior of the fiber-reinforced solid are characterized by *incompressible*, *transversely isotropic* stored-energy functions, with the same symmetry axis $\mathbf{N}$, of the *same separable* functional form:

$$W(\mathbf{F}) = \Psi(I_1, I_4) = \mathcal{F}(I_1) + \mathcal{G}(I_4). \tag{67}$$

Here, it is recalled (see Sect. 3.3.3) that $I_1 = \mathbf{F} \cdot \mathbf{F}$, $I_4 = \mathbf{FN} \cdot \mathbf{FN}$, and $\mathcal{F} : [3, \infty) \to [0, \infty)$ and $\mathcal{G} : (0, \infty) \to [0, \infty)$ are twice-differentiable, *convex* functions of their arguments satisfying the standard linearization conditions $\mathcal{F}(3) = \mathcal{F}'(3) = 0$ and $\mathcal{G}(1) = \mathcal{G}'(1) = 0$, so that

$$\mathcal{F}'(I_1) > 0, \quad \mathcal{F}''(I_1) \geq 0 \quad \forall\, I_1 > 3, \tag{68}$$

and

$$\mathcal{G}'(I_4) > 0\,(< 0) \quad \forall\, I_4 > 1\,(< 1), \quad \mathcal{G}''(I_4) \geq 0 \quad \forall\, I_4 > 0, \tag{69}$$

where the primes denote differentiation with respect to the appropriate argument (e.g., $\mathcal{F}'(\cdot) = \mathrm{d}\mathcal{F}(\cdot)/\mathrm{d}I_1$, $\mathcal{F}''(\cdot) = \mathrm{d}^2\mathcal{F}(\cdot)/\mathrm{d}{I_1}^2$). Physically, note that the function $\mathcal{F}$ characterizes the "soft" modes of deformation of this class of transversely isotropic materials, while $\mathcal{G}$ measures the "hard" modes. For notational simplicity, note further that expressions (67)–(69) have been written in generic form, in the sense that by adding the superscript (2), they refer to the fibers and that by adding overbars, they refer to the fiber-reinforced solid.

The loss of strong ellipticity[8] of the stored-energy function (67), as worked out next, can be computed in closed form. This will allow to also write down in closed form the relevant specialization of the onset-of-failure condition (66) in the next section. We begin by spelling out the condition of strong ellipticity for the stored-energy function (67):

$$\min_{\substack{||\mathbf{u}||=||\mathbf{v}||=1 \\ \mathbf{u}\cdot\mathbf{v}=0}} Q\,(\mathbf{u}, \mathbf{v}; \mathbf{F}) > 0, \tag{70}$$

[8] In an earlier effort, Merodio and Ogden [44] have studied the loss of strong ellipticity of stored-energy functions of the form (67) in the special case of plane-strain conditions, with the fiber direction lying in the plane of deformation.

where

$$Q(\mathbf{u},\mathbf{v};\mathbf{F}) = 4\mathcal{F}''(I_1)\left(\mathbf{u}^*\cdot\mathbf{v}^*\right)^2 + 2\mathcal{F}'(I_1)\left[\mathbf{u}^*\cdot\mathbf{u}^* - (\mathbf{N}\cdot\mathbf{u}^*)^2\right] + 2\left(\mathbf{N}\cdot\mathbf{u}^*\right)^2\left[\mathcal{F}'(I_1)+\mathcal{G}'(I_4)+2\mathcal{G}''(I_4)\left(\mathbf{N}\cdot\mathbf{v}^*\right)^2\right] \tag{71}$$

with $\mathbf{u}^* = \mathbf{F}^T\mathbf{u}$ and $\mathbf{v}^* = \mathbf{F}^T\mathbf{v}$, and it is emphasized that the unit vectors $\mathbf{u}$ and $\mathbf{v}$ in (70) satisfy the incompressibility constraint $\mathbf{u}\cdot\mathbf{v} = 0$. Given the inequalities (68), (69), $(\mathbf{u}^*\cdot\mathbf{v}^*)^2 \geq 0$, $\mathbf{u}^*\cdot\mathbf{u}^* > 0$, $(\mathbf{N}\cdot\mathbf{u}^*)^2 \geq 0$, $\mathbf{u}^*\cdot\mathbf{u}^* - (\mathbf{N}\cdot\mathbf{u}^*)^2 \geq 0$, and $(\mathbf{N}\cdot\mathbf{v}^*)^2 \geq 0$, it is then a simple matter to conclude that: *along an arbitrary loading path with starting point* $\mathbf{F} = \mathbf{I}$, *condition* (64) *is first violated* (i.e., $Q = 0$) *at critical deformation gradients* $\mathbf{F}_{\rm cr}$ *that are solution of the invariant equation*

$$\mathcal{F}'(I_1^{\rm cr}) + \mathcal{G}'(I_4^{\rm cr}) = 0, \tag{72}$$

where $I_1^{\rm cr} = \mathbf{F}_{\rm cr}\cdot\mathbf{F}_{\rm cr}$ *and* $I_4^{\rm cr} = \mathbf{F}_{\rm cr}\mathbf{N}\cdot\mathbf{F}_{\rm cr}\mathbf{N}$. Moreover, the associated critical vectors are given by

$$\mathbf{u}_{\rm cr} = \left\|\mathbf{F}_{\rm cr}^{-T}\mathbf{N}\right\|^{-1}\mathbf{F}_{\rm cr}^{-T}\mathbf{N} \tag{73}$$

and

$$\mathbf{v}_{\rm cr} = \left\|(\mathbf{F}_{\rm cr}\mathbf{N})\times\left(\mathbf{F}_{\rm cr}^{-T}\mathbf{N}\right)\right\|^{-1}(\mathbf{F}_{\rm cr}\mathbf{N})\times\left(\mathbf{F}_{\rm cr}^{-T}\mathbf{N}\right). \tag{74}$$

A few theoretical and practical remarks regarding this result are in order:

- If the functions $\mathcal{F}$ and $\mathcal{G}$ are such that there is no pair of real numbers $(I_1^{\rm cr}, I_4^{\rm cr})$ in the physically admissible intervals, $I_1^{\rm cr} \in [I_4^{\rm cr} + 2/\sqrt{I_4^{\rm cr}}, \infty)$ and $I_4^{\rm cr} \in (0,\infty)$, that satisfy the nonlinear algebraic equation (72), then loss of strong ellipticity does not occur. In the event that loss of strong ellipticity does occur, the set of points that first satisfy condition (72) along an arbitrary loading path with starting point $(I_1, I_4) = (3, 1)$ defines a "failure curve" $\mathcal{C}(I_1, I_4) = 0$ in (I_1, I_4)–space.
- Loss of strong ellipticity may only occur when the deformation in the "fiber" direction $\mathbf{N}$, as measured by I_4, reaches a sufficiently large *compressive* value, since (in view of the inequalities (68) and (69)) only for deformations $\mathbf{F}_{\rm cr}$ with $I_4^{\rm cr} \leq 1$ Eq. 72 admits physical solutions.
- The vector (73) defining the orientation of weak surfaces where the deformation may localize is seen to correspond to the image in the deformed configuration of the initial "fiber" direction $\mathbf{N}$ when treated not as a material line element, but as the normal to a material surface. Moreover, the vector (74) is perpendicular to the direction of the "fibers" in the deformed configuration, $\mathbf{n} = \mathbf{F}_{\rm cr}\mathbf{N}$, and, of course, also perpendicular to (73), as a result of the macroscopic incompressibility constraint.
- Physically, it is important to recognize that the function $\mathcal{G}'$ measures the "hard" mode of deformation of the transversely isotropic material, whereas the function $\mathcal{F}'$ measures the "soft" mode. Thus, condition (72) states rather interestingly that transversely isotropic materials (characterized by stored-energy functions of the form (67)) may develop instabilities whenever the *compressive* deformation in the "fiber" direction $\mathbf{N}$, as measured by I_4, reaches a certain critical value determined by the ratio of "hard"-to-"soft" modes of deformation $\mathcal{G}'(I_4)/\mathcal{F}'(I_1)$.

6 Application to Neo-Hookean solids reinforced with anisotropic fibers

As a first effort to derive constitutive models for fiber-reinforced hyperelastic solids via the Hamilton–Jacobi formulation (33), we consider the physically relevant case of material systems made up of an incompressible Neo-Hookean solid with stored-energy function

$$W^{(1)}(\mathbf{F}) = \Psi^{(1)}(I_1) = \frac{\mu^{(1)}}{2}(I_1 - 3) \tag{75}$$

reinforced by a random and transversely isotropic distribution of *transversely isotropic* fibers with incompressible stored-energy function

$$W^{(2)}(\mathbf{F}) = \Psi^{(2)}(I_1, I_4) = \frac{\mu_n^{(2)}}{2}(I_1 - 3) + g^{(2)}(I_4). \tag{76}$$

Here, the positive material parameters $\mu^{(1)}$ and $\mu_n^{(2)}$ denote, respectively, the shear modulus of the (isotropic) matrix phase and the longitudinal shear modulus of the (transversely isotropic) fibers in the ground state. Moreover, $g^{(2)} : (0, \infty) \to [0, \infty)$ is a twice-differentiable *convex* function that satisfies the typical undeformed-configuration conditions:

$$g^{(2)}(1) = \frac{\mathrm{d}g^{(2)}}{\mathrm{d}I_4}(1) = 0, \quad \frac{\mathrm{d}^2 g^{(2)}}{\mathrm{d}I_4^2}(1) = \frac{3}{4}\left(\mu_a^{(2)} - \mu_n^{(2)}\right), \tag{77}$$

where the positive material constant $\mu_a^{(2)} \geq \mu_n^{(2)}$ corresponds to the axisymmetric shear modulus of the fibers in the ground state. An example of the form (76) which has been recently proposed in the literature [9] (to model, for instance, collagen fibers) is

$$\Psi^{(2)}(I_1, I_4) = \frac{\mu_n^{(2)}}{2}(I_1 - 3) - \frac{3(\mu_a^{(2)} - \mu_n^{(2)})}{8} J_m \ \ln\left[1 - \frac{(I_4 - 1)^2}{J_m}\right], \tag{78}$$

where the parameter J_m serves to measure the limiting chain extensibility of the fibers, i.e., the fibers lock up at $I_4 = \sqrt{J_m} + 1$. Note that in the limit as $J_m \to \infty$, expression (78) reduces to the standard reinforcing model

$$\Psi^{(2)}(I_1, I_4) = \frac{\mu_n^{(2)}}{2}(I_1 - 3) + \frac{3(\mu_a^{(2)} - \mu_n^{(2)})}{8}(I_4 - 1)^2. \tag{79}$$

Given (75) and (76), together with the help of the non-dimensional stored-energy function

$$\hat{\Psi}(\overline{I}_1, \overline{I}_2, \overline{I}_4, \overline{I}_5, c_0) = \frac{1}{\mu^{(1)}}\overline{\Psi}(\overline{I}_1, \overline{I}_2, \overline{I}_4, \overline{I}_5, c_0) - \frac{1}{2}(\overline{I}_1 - 3), \tag{80}$$

the relevant Hamilton–Jacobi equation (48) can be shown (see Appendix C) to specialize simply to

$$\begin{aligned} c_0 \frac{\partial \hat{\Psi}}{\partial c_0} - \hat{\Psi} - \left(\overline{I}_1 - \overline{I}_4 - \frac{2}{\sqrt{\overline{I}_4}}\right)\left(\frac{\partial \hat{\Psi}}{\partial \overline{I}_1}\right)^2 - h_{22}\left(\frac{\partial \hat{\Psi}}{\partial \overline{I}_2}\right)^2 - h_{55}\left(\frac{\partial \hat{\Psi}}{\partial \overline{I}_5}\right)^2 - h_{12}\frac{\partial \hat{\Psi}}{\partial \overline{I}_1}\frac{\partial \hat{\Psi}}{\partial \overline{I}_2} - h_{15}\frac{\partial \hat{\Psi}}{\partial \overline{I}_1}\frac{\partial \hat{\Psi}}{\partial \overline{I}_5} \\ - h_{25}\frac{\partial \hat{\Psi}}{\partial \overline{I}_2}\frac{\partial \hat{\Psi}}{\partial \overline{I}_5} = 0, \end{aligned} \tag{81}$$

subject to the initial condition

$$\hat{\Psi}(\overline{I}_1, \overline{I}_2, \overline{I}_4, \overline{I}_5, 1) = \frac{1}{2}\left(\frac{\mu^{(2)}}{\mu^{(1)}} - 1\right)(\overline{I}_1 - 3) + \frac{1}{\mu^{(1)}} g^{(2)}(\overline{I}_4). \tag{82}$$

The coefficients h_{ij} in (81) are functions of the invariants $\overline{I}_1, \overline{I}_2, \overline{I}_4$, and $\overline{I}_5$. However, because the coefficient multiplying $\partial\hat{\Psi}/\partial\overline{I}_1$ in (81) and the initial condition (82) depend on $\overline{I}_1$ and $\overline{I}_4$ *only*, it follows that the solution $\hat{\Psi}$ is *independent* of $\overline{I}_2$ and $\overline{I}_5$, the derivatives $\partial\hat{\Psi}/\partial\overline{I}_2$ and $\partial\hat{\Psi}/\partial\overline{I}_5$ are zero, and the coefficients h_{ij} are thus irrelevant. The simplified differential equation for $\hat{\Psi}$ admits a *closed-form* solution that ultimately leads to

$$\overline{\Psi}(\overline{I}_1, \overline{I}_4, c_0) = \frac{\widetilde{\mu}}{2}(\overline{I}_1 - 3) + \frac{\overline{\mu}_n - \widetilde{\mu}}{2}\frac{\left(\sqrt{\overline{I}_4} + 2\right)\left(\sqrt{\overline{I}_4} - 1\right)^2}{\sqrt{\overline{I}_4}} + c_0 g^{(2)}(\overline{I}_4), \tag{83}$$

where

$$\overline{\mu}_n = (1 - c_0)\mu^{(1)} + c_0\mu_n^{(2)} \tag{84}$$

and

$$\widetilde{\mu} = \frac{(1-c_0)\mu^{(1)} + (1+c_0)\mu_n^{(2)}}{(1+c_0)\mu^{(1)} + (1-c_0)\mu_n^{(2)}}\,\mu^{(1)}. \tag{85}$$

Expression (83) constitutes an exact stored-energy function for the macroscopic response of Neo-Hookean solids (75) reinforced by a random and transversely isotropic distribution of anisotropic fibers of the form (76) with volume fraction c_0.

Below are a few theoretical and practical remarks regarding the above-derived result:

(i) In the limit of small deformations as $\overline{\mathbf{F}} \to \mathbf{I}$ (so that $\overline{I}_1 \to 3$ and $\overline{I}_4 \to 1$), the stored-energy function (83) reduces to

$$\overline{\Psi} = \frac{\widetilde{\mu}_p + \widetilde{\mu}_n}{2}\left(\mathrm{tr}\overline{\boldsymbol{\varepsilon}}^2 - \frac{3}{2}(\mathbf{N}\cdot\overline{\boldsymbol{\varepsilon}}\mathbf{N})^2\right) + \widetilde{\mu}_a\frac{3}{2}(\mathbf{N}\cdot\overline{\boldsymbol{\varepsilon}}\mathbf{N})^2 + O\left(||\overline{\mathbf{F}}-\mathbf{I}||^3\right), \tag{86}$$

where $\overline{\boldsymbol{\varepsilon}} = (\overline{\mathbf{F}} + \overline{\mathbf{F}}^T - 2\mathbf{I})/2$ is the infinitesimal strain tensor, and

$$\widetilde{\mu}_p = \widetilde{\mu}_n = \widetilde{\mu}, \quad \text{and} \quad \widetilde{\mu}_a = (1-c_0)\mu^{(1)} + c_0\mu_a^{(2)} \tag{87}$$

are, respectively, the three shear moduli that characterize the transverse, longitudinal, and axisymmetric shear response of the (incompressible, transversely isotropic) fiber-reinforced material in the ground state. Note that the transverse and longitudinal shear moduli, as given by expressions $(87)_1$ and (85), are identical to each other and agree exactly with the Hashin–Shtrikman (HS) *optimal lower bound* for the transverse and longitudinal shear moduli of transversely isotropic materials with linearly elastic incompressible constituents (see, e.g., [45]). On the other hand, the axisymmetric shear modulus, as given by expression $(87)_2$, is seen to be nothing more than the Voigt *optimal upper bound* (see, e.g., [45]). In the further limit of dilute concentrations of fibers ($c_0 \to 0$), the result (86) reduces to the relevant Eshelby solution for the problem of a single fiber of circular cross-section embedded in an infinite matrix.

(ii) In the finite-deformation regime, expression (83) is seen to be bounded from above (recall that $\overline{I}_1 \geq \overline{I}_4 + 2/\sqrt{\overline{I}_4}$) by the rigorous Voigt upper bound:

$$\overline{\Psi}_V = \frac{\overline{\mu}_n}{2}(\overline{I}_1 - 3) + c_0 g^{(2)}(\overline{I}_4). \tag{88}$$

Note that (88), which is the only known non-trivial bound for the type of fiber-reinforced materials of interest in this work, depends on the microstructure only through the volume fraction of the fibers c_0. In general, the stored-energy function (88) is expected to be too stiff. However, as already mentioned, for the special case of axisymmetric shear loading aligned with the fibers, i.e., $\overline{I}_1 = \overline{I}_4 + 2/\sqrt{\overline{I}_4}$, the Voigt bound is an *exact* result (see the work [41] for a general discussion on uniform-field exact solutions in fiber-reinforced hyperelastic solids) to which the *realizable* stored-energy function (82) reduces, of course.

(iii) The effective stored-energy function (83) depends only on the invariants $\overline{I}_1, \overline{I}_4$, and *not* on $\overline{I}_2, \overline{I}_5$. Furthermore its functional structure is separable like that of the underlying fibers (76), namely,

$$\overline{\Psi} = \mathcal{F}(\overline{I}_1) + \mathcal{G}(\overline{I}_4), \tag{89}$$

where

$$\mathcal{F}(\overline{I}_1) = \frac{\widetilde{\mu}}{2}\left(\overline{I}_1 - 3\right) \tag{90}$$

and

$$\mathcal{G}(\overline{I}_4) = \frac{\overline{\mu}_n - \widetilde{\mu}}{2}\frac{\left(\sqrt{\overline{I}_4}+2\right)\left(\sqrt{\overline{I}_4}-1\right)^2}{\sqrt{\overline{I}_4}} + c_0 g^{(2)}(\overline{I}_4) \tag{91}$$

are *convex* functions of their arguments. From a physical point of view, note that the parameter $\widetilde{\mu}$ in (90) characterizes the matrix-dominated ("soft") modes of deformation of the fiber-reinforced material, while the parameter $\overline{\mu}_n$ and the function $g^{(2)}$ in (91) characterize the fiber-dominated ("hard") modes, and that these

"soft" and "hard" modes are uncoupled. In passing, it is relevant to emphasize that for the more general case of matrix constituents that are *not* Neo-Hookean, the homogenized response defined by (48) can be shown to depend on all the invariants $\overline{I}_1$, $\overline{I}_2$, $\overline{I}_4$, and $\overline{I}_5$ (irrespectively of the constitutive behavior of the fibers) and *not* to be of the separable form $\overline{\Psi} = \mathcal{F}_{\rm iso}(\overline{I}_1, \overline{I}_2) + \mathcal{G}_{\rm fib}(\overline{I}_4, \overline{I}_5)$, as often assumed in the literature (see, e.g., [9] and references therein) on a purely phenomenological basis.

(iv) When the fibers are taken to be simply Neo-Hookean (i.e., $g^{(2)} = 0$), the stored-energy function (83) reduces identically to the *estimate* recently proposed by deBotton et al. [12]. The reason for this agreement hinges upon the fact that these authors constructed their model under the main simplifying assumption that the transverse, longitudinal, and axisymmetric modes of deformation are uncoupled, which according to the exact Hamilton–Jacobi formulation (83) happens to be the case when both the matrix and fibers are Neo-Hookean.

(v) While exact for a specific microstructure with fibers of polydisperse sizes, we conjecture that (83) is actually a *rigorous lower bound* for the effective stored-energy functions of Neo-Hookean solids (75) reinforced by a transversely isotropic distribution of anisotropic fibers with stored-energy function (76), at least before the onset of any instability. This conjecture is primarily based on the observation that, for any applied macroscopic loading $\overline{\mathbf{F}}$, the fibers undergo locally a *uniform* deformation; such class of deformations is usually associated with the softest possible response of stiff materials (e.g., [46]). Note that remark *i* above directly supports that the stored-energy function (83) indeed constitutes a lower bound.

(vi) By construction, the stored-energy function (83) is expected to be reasonably accurate for the macroscopic response of Neo-Hookean solids reinforced by a transversely isotropic distribution of circular fibers with a very wide distribution of diameters for the *entire range* of volume fractions $c_0 \in [0, 1]$. More specifically, for matrix-dominated modes of deformation (e.g., transverse and longitudinal shear) the result (83) is expected to be accurate but somewhat soft, in view of its conjectured status of lower bound (see, e.g., [47] for comparisons with full-field simulations for Neo-Hookean solids reinforced by a random and transversely isotropic distribution of monodisperse circular fibers under transverse shear deformations). For fiber-dominated modes of deformation (e.g., axisymmetric shear), on the other hand, the result (83) is expected to be very accurate, in accordance with the microstructure-independent Voigt bound (88) which, again, is exact for aligned axisymmetric shear loading conditions.

6.1 Onset of instabilities

Next, we study in detail the development of instabilities in fiber-reinforced solids characterized by the stored-energy function (83) under *completely general loading conditions*, in light of the general discussion of Sect. 5.

After direct substitution of expressions (76) and (83) in the onset-of-failure condition (66), with the help of relation (60) and condition (72), it is a simple matter to deduce that: *along an arbitrary loading path with starting point* $\overline{\mathbf{F}} = \mathbf{I}$, *the stored-energy function* (83) *first becomes unstable at critical deformations* $\overline{\mathbf{F}}_{\rm cr}$ *with* $\overline{I}_4^{\rm cr} = \overline{\mathbf{F}}_{\rm cr}\mathbf{N} \cdot \overline{\mathbf{F}}_{\rm cr}\mathbf{N}$ *that satisfy*

$$\frac{\mu_n^{(2)}}{2} + \frac{{\rm d}g^{(2)}}{{\rm d}\overline{I}_4}(\overline{I}_4^{\rm cr}) = 0 \quad \text{or} \quad \overline{I}_4^{\rm cr} = \left[1 + \frac{2c_0}{\overline{\mu}_n}\frac{{\rm d}g^{(2)}}{{\rm d}\overline{I}_4}(\overline{I}_4^{\rm cr})\right]^{-2/3}\left(1 - \frac{\widetilde{\mu}}{\overline{\mu}_n}\right)^{2/3}. \tag{92}$$

Moreover, the associated critical vectors $\mathbf{u}_{\rm cr}$ and $\mathbf{v}_{\rm cr}$ that describe how the material loses strong ellipticity at $\overline{\mathbf{F}}_{\rm cr}$ are given by expressions (73) and (74). Here, it is recalled that $\overline{\mu}_n$ and $\widetilde{\mu}$ are given, respectively, by expressions (84) and (85) in terms of the shear moduli $\mu^{(1)}$ and $\mu_n^{(2)}$ of the matrix and fiber phases, and of the volume fraction of fibers c_0.

In a physical sense, as already pointed out in the more general context of Sect. 5, if condition $(92)_1$ is satisfied, the fibers fail locally. On the other hand, if condition $(92)_2$ is met, then a macroscopic instability may develop. Note that the onset of instabilities occur only when the deformation along the fiber direction, as measured by the

invariant $\overline{I}_4$, is of a sufficiently large *compressive*[9] value $\overline{I}_4 = \overline{I}_4^{\rm cr} \leq 1$ determined by certain ratios between the hard and soft modes of deformation. Indeed, as already described in remark *iii* above, the parameters $\mu_n^{(2)}$ and $\widetilde{\mu}$ characterize, respectively, the soft modes of deformation of the fibers and of the fiber-reinforced material, while $\mathrm{d}g^{(2)}/\mathrm{d}\overline{I}_4$ and $\overline{\mu}_n$ characterize their hard modes. From a computational point of view, it is also worth remarking that the nonlinear algebraic equations $(92)_1$ and $(92)_2$ cannot be solved explicitly for $\overline{I}_4^{\rm cr}$ in general. For the special case when the fibers are taken to be Neo-Hookean (i.e., $g^{(2)} = 0$), however, $(92)_1$ is clearly never satisfied since $\mu_n^{(2)} > 0$ and equation $(92)_2$ leads to

$$\overline{I}_4^{\rm cr} = \left(1 - \frac{\widetilde{\mu}}{\overline{\mu}_n}\right)^{2/3}. \tag{93}$$

This explicit result shows particulary well that the onset of instabilities is indeed controlled by the ratio of hard-to-soft modes of deformation (given here by $\widetilde{\mu}/\overline{\mu}_n$).

6.2 The case of nearly rigid fibers

Criterion (92) applies to general heterogeneity contrast between the matrix and the fibers. In practice, however, actual fibers in reinforced soft materials are usually several orders of magnitude stiffer than the matrix phase. In this regard, it is convenient to spell out the specialization of the above result in the limit as the fibers are taken to be rigid. To this end, we begin by recognizing that the stored-energy function (76) characterizing the behavior of the fibers admits the following asymptotic representation

$$\Psi^{(2)}(I_1, I_4) = \frac{\mu_n^{(2)}}{2}(I_1 - 3) + \frac{1}{2}\frac{\mathrm{d}g^{(2)}}{\mathrm{d}I_4}(1)\,(I_4 - 1)^2 + O\left((I_4 - 1)^3\right), \tag{94}$$

where

$$\frac{\mathrm{d}g^{(2)}}{\mathrm{d}I_4}(1) = \frac{3}{4}\left(\mu_a^{(2)} - \mu_n^{(2)}\right), \tag{95}$$

and subsequently define the parameters

$$\delta = \frac{\mu^{(1)}}{\mu_a^{(2)}} \quad \text{and} \quad \delta_f = \frac{\mu_n^{(2)}}{\mu_a^{(2)}}, \tag{96}$$

which serve to measure, respectively, the heterogeneity contrast between the matrix and the fibers (in the fiber direction), and the fiber anisotropy.

Fixing now the values of δ_f, $\mu^{(1)}$, and c_0, it is a simple to matter to show that the failure criterion (92) for the critical invariant $\overline{I}_4^{\rm cr}$ at which the fiber-reinforced material becomes unstable reduces asymptotically to

$$\delta_f \mu^{(1)} + 2\delta \frac{\mathrm{d}g^{(2)}}{\mathrm{d}\overline{I}_4^{\rm cr}}(\overline{I}_4^{\rm cr}) = 0 \quad \text{or} \quad \overline{I}_4^{\rm cr} = 1 - \frac{2(1 + c_0)}{3c_0(1 - c_0)}\,\delta + O(\delta^2) \tag{97}$$

in the limit as $\delta \to 0$, namely, in the limit as the fibers are made infinitely stiff in the fiber direction with respect to the matrix. Of course, for the case of exactly rigid fibers ($\delta = 0$), the fiber-reinforced material is already unstable at $\overline{I}_4^{\rm cr} = 1$, as readily deduced from the macroscopic condition $(97)_2$. To first order in δ, it is also plain that the macroscopic condition $(97)_2$, and *not* the local fiber condition $(97)_1$, is the failure condition that will be satisfied first, except in the limiting cases when $c_0 = 0$ and $c_0 = 1$. In this regard, it is interesting to notice that, to first order in δ, the critical invariant $\overline{I}_4^{\rm cr}$ determined by $(97)_2$ does not depend on the longitudinal shear modulus $\mu_n^{(2)}$. That is, in the case of very stiff fibers in the fiber direction ($\mu_a^{(2)} \gg 1$), the onset of macroscopic instabilities is entirely independent of the longitudinal (and transverse) stiffness of the fibers, and the only heterogeneity parameter that matters is the stiffness contrast in the fiber direction between the fibers and the matrix.

[9] Recall that $\mathrm{d}g^{(2)}(\overline{I}_4^{\rm cr})/\mathrm{d}\overline{I}_4 > 0 (< 0)$ for $\overline{I}_4^{\rm cr} > 1 (< 1)$ and $\overline{\mu}_n \geq \widetilde{\mu} > 0$, so that $\overline{I}_4^{\rm cr}$ in (92) is necessarily less than or equal to 1.

7 Final remarks

We have proposed a novel homogenization-based constitutive theory for fiber-reinforced hyperelastic solids with *random* microstructures. The theory incorporates microstructural information in the form of one- and two-point probabilities, and is general enough to allow for any matrix and fiber stored-energy functions, and completely general loading conditions. Moreover, it has the distinguishing virtue of being *realizable*, in the sense that it reproduces exactly the behavior of material systems with a certain class of microgeometries. Consequently, the resulting effective stored-energy function is guaranteed to be objective, to satisfy all pertinent bounds, to linearize properly, to be exact to second order in the heterogeneity contrast, and to comply with any macroscopic constraints imposed by microscopic constraints, such as the strongly nonlinear constraint of incompressibility. The proposed formulation also grants access to information on the distribution of the local fields within each phase, which is required to characterize the evolution of microstructure and the onset of instabilities. With the possible exception of the "linear comparison" theory [31], none of the existing constitutive theories for fiber-reinforced hyperelastic solids exhibits such degree of generality and satisfies the above theoretical requirements simultaneously.

From a computational point of view, the proposed macroscopic stored-energy functions are solution to a nonlinear Hamilton–Jacobi equation, viz. Eq. 33, with the fiber concentration and macroscopic deformation gradient playing the role of "time" and "space", respectively. In general, the underlying Hamiltonians, viz. Eq. 34, may not admit closed-form representations, in which case the Hamilton–Jacobi equation may have to be solved numerically. Fortunately, a substantial body of literature exists on efficient techniques for solving Hamilton–Jacobi equations, especially on the method of characteristics (see, e.g., [37]), due to the prominent role of this type of equations in physics. In addition, approximate solutions that are computationally efficient may result from the use of variational formulations of Hamilton–Jacobi equations; see, for instance, [48, Chaps. III and IV].

As a first application, the theory was used to generate results for a physically relevant class of material systems consisting of a Neo-Hookean matrix reinforced with *anisotropic* fibers. A *closed-form* effective stored-energy function was obtained for general three-dimensional loading conditions, namely expression (83). In addition, an *analytical* expression (92) for the associated onset-of-failure surface was provided. This surface accounts for two failure mechanisms: local fiber instabilities and macroscopic, or long wavelength, instabilities. However, other local mechanisms that are precursors of failure can also be incorporated to the proposed formulation. Two notable examples are fiber debonding and matrix cavitation. Failure surfaces that account for all these mechanisms simultaneously are of great practical importance and efforts to determine them are currently under way.

We conclude this work by mentioning that a similar strategy has been used to develop a constitutive theory for more general two-phase material systems, such as particle-reinforced and porous solids, which will be reported in a forthcoming publication [42].

Appendix A: Hamiltonian for infinitesimal deformations

In this appendix we compute the specialization of the Hamiltonian (34) in the limit as $\overline{\mathbf{F}} \to \mathbf{I}$. We begin by recalling that in the limit of small deformations, the local and effective stored-energy functions take, respectively, the asymptotic forms (1) and (37). It then follows that the leading order term of the optimality condition with respect to $\boldsymbol{\omega}$ in (34) is simply

$$\left[\boldsymbol{\mathcal{L}}_0^{(2)}\overline{\boldsymbol{\varepsilon}} - \widetilde{\boldsymbol{\mathcal{L}}}_0(\overline{\boldsymbol{\varepsilon}} + \boldsymbol{\omega}\otimes\boldsymbol{\xi})\right]\boldsymbol{\xi} = \mathbf{0}, \tag{98}$$

which can be solved explicitly to render

$$\boldsymbol{\omega}\otimes\boldsymbol{\xi} = \boldsymbol{\mathcal{Q}}(\boldsymbol{\xi})\Delta\widetilde{\boldsymbol{\mathcal{L}}}\overline{\boldsymbol{\varepsilon}}. \tag{99}$$

Here, $\Delta\widetilde{\boldsymbol{\mathcal{L}}}_0 \equiv \widetilde{\boldsymbol{\mathcal{L}}}_0 - \boldsymbol{\mathcal{L}}_0^{(1)}$ and $\boldsymbol{\mathcal{Q}}(\boldsymbol{\xi})$ is a fourth-order tensor with components $\mathcal{Q}_{ijkl} = K_{ik}^{-1}\xi_j\xi_l$, $K_{ik} = \mathcal{L}_{0\,ijkl}^{(1)}\xi_j\xi_l$. The Hamiltonian (34) is then seen to be given by

$$H\left(\overline{\mathbf{F}},\overline{W},\frac{\partial\overline{W}}{\partial\overline{\mathbf{F}}}\right)=\frac{1}{2}\overline{\boldsymbol{\varepsilon}}\cdot\left[\Delta\widetilde{\mathcal{L}}+\Delta\widetilde{\mathcal{L}}\mathcal{P}\Delta\widetilde{\mathcal{L}}\right]\overline{\boldsymbol{\varepsilon}}+O\left(||\overline{\mathbf{F}}-\mathbf{I}||^3\right),\tag{100}$$

where $\mathcal{P}$ is the microstructural tensor defined as

$$\mathcal{P}=\langle\mathcal{Q}\rangle=\int\limits_{|\boldsymbol{\xi}|=1}\mathcal{Q}(\boldsymbol{\xi})\nu(\boldsymbol{\xi})\mathrm{d}\boldsymbol{\xi}.\tag{101}$$

Appendix B: Hamiltonian for incompressible transversely isotropic solids under axisymmetric loading

Under aligned axisymmetric isochoric loadings (i.e., $\overline{I}_1=\overline{I}_4+2/\sqrt{\overline{I}_4}$, $\overline{I}_2=2\sqrt{\overline{I}_4}+1/\overline{I}_4$, $\overline{I}_3=1$, and $\overline{I}_5=\overline{I}_4^2$), the macroscopic deformation gradient and stress tensors admit the representations

$$\overline{\mathbf{F}}=\overline{\lambda}_N\mathbf{N}\otimes\mathbf{N}+\overline{\lambda}_N^{-1/2}\left(\boldsymbol{\xi}\otimes\boldsymbol{\xi}+\boldsymbol{\xi}^{\perp}\otimes\boldsymbol{\xi}^{\perp}\right),\tag{102}$$

$$\overline{\mathbf{S}}=\overline{S}_N\mathbf{N}\otimes\mathbf{N}+\overline{S}_p\left(\boldsymbol{\xi}\otimes\boldsymbol{\xi}+\boldsymbol{\xi}^{\perp}\otimes\boldsymbol{\xi}^{\perp}\right),\tag{103}$$

where $\overline{S}_N$ and $\overline{S}_p$ denote the axial and in-plane stresses, and $\overline{\lambda}_N\equiv\sqrt{\overline{I}_4}>0$ denotes the axisymmetric stretch. Macroscopic incompressibility requires that the optimal $\boldsymbol{\omega}$ in the Hamiltonian (34) be of the form (43); in view of (102) we can write

$$\boldsymbol{\omega}\otimes\boldsymbol{\xi}=\omega_N\overline{\lambda}_N\mathbf{N}\otimes\boldsymbol{\xi}+\omega_{\perp}\overline{\lambda}_N^{-1/2}\boldsymbol{\xi}^{\perp}\otimes\boldsymbol{\xi}.\tag{104}$$

It is evident that the scalar product between the tensors (103) and (104) is zero. Thus, the Hamiltonian (34) reduces to

$$H=\overline{\Psi}-\min_{\omega_N,\,\omega_{\perp}}\left\langle\Psi^{(1)}\left(I_1^{(1)},I_2^{(1)},I_4^{(1)},I_5^{(1)}\right)\right\rangle,\tag{105}$$

where the $I_\alpha^{(1)}$'s denote the transversely isotropic incompressible invariants associated with the tensor $(\overline{\mathbf{F}}+\boldsymbol{\omega}\otimes\boldsymbol{\xi})$:

$$I_1^{(1)}=[2+\overline{\lambda}_N^3(1+\omega_N^2)+\omega_{\perp}^2]/\overline{\lambda}_N,\quad I_2^{(1)}=\overline{\lambda}_N^{-2}+\overline{\lambda}_N(2+\omega_N^2+\omega_{\perp}^2),\quad I_4^{(1)}=\overline{\lambda}_N^2,\quad I_5^{(1)}=\overline{\lambda}_N^4(1+\omega_N^2).\tag{106}$$

These invariants are all monotonically increasing functions of ω_N and $\omega_{\perp}$. Now, commonly used energies $\Psi^{(1)}$ are convex functions of the four invariants (106). In that case, the minimum in (105) is attained at $\omega_N=\omega_{\perp}=0$, and the Hamiltonian reduces to

$$H=\overline{\Psi}-\Psi^{(1)}(\overline{I}_1,\overline{I}_2,\overline{I}_4,\overline{I}_5),\tag{107}$$

where the $\overline{I}_\alpha$'s denote the four transversely isotropic incompressible invariants of $\overline{\mathbf{C}}=\overline{\mathbf{F}}^T\overline{\mathbf{F}}$.

Appendix C: Hamiltonian for fiber-reinforced Neo-Hookean solids

Macroscopic incompressibility requires that the optimal vector $\boldsymbol{\omega}$ be the form (43). Optimizing with respect to the components $\omega_N(\boldsymbol{\xi})$ and $\omega_{\perp}(\boldsymbol{\xi})$ leads to a system of two linear equations:

$$\frac{\partial\overline{\Psi}}{\partial\overline{\mathbf{F}}}\cdot(\overline{\mathbf{F}}\mathbf{N}\otimes\boldsymbol{\xi})-\mu^{(1)}\left(\overline{\mathbf{F}}+\boldsymbol{\omega}\otimes\boldsymbol{\xi}\right)\cdot(\overline{\mathbf{F}}\mathbf{N}\otimes\boldsymbol{\xi})=0,\tag{108}$$

$$\frac{\partial\overline{\Psi}}{\partial\overline{\mathbf{F}}}\cdot(\overline{\mathbf{F}}\boldsymbol{\xi}^{\perp}\otimes\boldsymbol{\xi})-\mu^{(1)}\left(\overline{\mathbf{F}}+\boldsymbol{\omega}\otimes\boldsymbol{\xi}\right)\cdot(\overline{\mathbf{F}}\boldsymbol{\xi}^{\perp}\otimes\boldsymbol{\xi})=0.\tag{109}$$

The solution to these equations can be conveniently written in terms of the non-dimensional function

$$\hat{\Psi}\equiv\frac{\overline{\Psi}}{\mu^{(1)}}-\frac{1}{2}(\overline{I}_1-3)\tag{110}$$

as

$$\boldsymbol{\omega} \otimes \boldsymbol{\xi} = \boldsymbol{\mathcal{M}}(\overline{\mathbf{F}}, \boldsymbol{\xi}) \frac{\partial \hat{\Psi}}{\partial \overline{\mathbf{F}}}. \tag{111}$$

In this expression, $\boldsymbol{\mathcal{M}}(\overline{\mathbf{F}}, \boldsymbol{\xi})$ is a fourth-order tensor with major symmetry, given by

$$\boldsymbol{\mathcal{M}}(\overline{\mathbf{F}}, \boldsymbol{\xi}) = \frac{1}{\sin^2 \alpha} \left[\mathbf{u}_N \otimes \mathbf{u}_N + \mathbf{u}_\perp \otimes \mathbf{u}_\perp - \cos\alpha \, (\mathbf{u}_N \otimes \mathbf{u}_\perp + \mathbf{u}_\perp \otimes \mathbf{u}_N) \right], \tag{112}$$

where

$$\mathbf{u}_N = \frac{\overline{\mathbf{F}}\mathbf{N} \otimes \boldsymbol{\xi}}{||\overline{\mathbf{F}}\mathbf{N} \otimes \boldsymbol{\xi}||}, \quad \mathbf{u}_\perp = \frac{\overline{\mathbf{F}}\boldsymbol{\xi}^\perp \otimes \boldsymbol{\xi}}{||\overline{\mathbf{F}}\boldsymbol{\xi}^\perp \otimes \boldsymbol{\xi}||}, \quad \cos\alpha = \mathbf{u}_N \cdot \mathbf{u}_\perp. \tag{113}$$

It is easy to show that the tensor $\boldsymbol{\mathcal{M}}$ satisfies the identity $\boldsymbol{\mathcal{M}}\boldsymbol{\mathcal{M}} = \boldsymbol{\mathcal{M}}$. Making use of this identity, it is then easy to show that the Hamiltonian (34) takes the form

$$H = \hat{\Psi} + \frac{1}{2} \frac{\partial \hat{\Psi}}{\partial \overline{\mathbf{F}}} \cdot \langle \boldsymbol{\mathcal{M}} \rangle \frac{\partial \hat{\Psi}}{\partial \overline{\mathbf{F}}}. \tag{114}$$

where the tensor

$$\langle \boldsymbol{\mathcal{M}} \rangle = \frac{1}{2\pi} \int\limits_{|\boldsymbol{\xi}|=1} \boldsymbol{\mathcal{M}}(\overline{\mathbf{F}}, \boldsymbol{\xi}) \, \mathrm{d}\boldsymbol{\xi} \tag{115}$$

is a function of the four transversely isotropic incompressible invariants of $\overline{\mathbf{C}} = \overline{\mathbf{F}}^T \overline{\mathbf{F}}$.

To carry out the integrals in (115), it is simplest to express the integrand in terms of a macroscopic deformation gradient of the form

$$\overline{F}_{ij} = \begin{bmatrix} \dfrac{1}{\sqrt{\overline{F}_{33}}} & 0 & 0 \\ \overline{F}_{21} & \dfrac{1}{\sqrt{\overline{F}_{33}}} & 0 \\ \overline{F}_{31} & \overline{F}_{32} & \overline{F}_{33} \end{bmatrix} \tag{116}$$

in a coordinate system $\mathbf{e}_i$ $(i = 1, 2, 3)$ with $\mathbf{e}_3 \equiv \mathbf{N}$. That $\overline{\mathbf{F}}$ can be restricted to be of this form follows from the overall transversely isotropic symmetry of the problem [49]. The four invariants $\overline{I}_1$, $\overline{I}_2$, $\overline{I}_4$, $\overline{I}_5$ are related to the four independent components in (116) as follows:

$$\begin{aligned} &\overline{I}_1 = \overline{F}_{33}^2 + \frac{2}{\overline{F}_{33}} + \overline{F}_{21}^2 + \overline{F}_{31}^2 + \overline{F}_{32}^2, \quad \overline{I}_2 = \frac{1}{\overline{F}_{33}^2} + \frac{\overline{F}_{31}^2 + \overline{F}_{32}^2}{\overline{F}_{33}} - \frac{2\overline{F}_{21}\overline{F}_{31}\overline{F}_{32}}{\sqrt{\overline{F}_{33}}} + 2\overline{F}_{33} + \overline{F}_{21}^2(\overline{F}_{32}^2 + \overline{F}_{33}^2), \\ &\overline{I}_4 = \overline{F}_{33}^2, \overline{I}_5 = \overline{F}_{33}^2 \left(\overline{F}_{31}^2 + \overline{F}_{32}^2 + \overline{F}_{33}^2 \right). \end{aligned} \tag{117}$$

Upon integrating (115) with (116), and making use of relations (117) to express the result in terms of the invariants, we obtain

$$\begin{aligned} H = \hat{\Psi} &+ \left(\overline{I}_1 - \overline{I}_4 - \frac{2}{\sqrt{\overline{I}_4}} \right) \left(\frac{\partial \hat{\Psi}}{\partial \overline{I}_1} \right)^2 + h_{22} \left(\frac{\partial \hat{\Psi}}{\partial \overline{I}_2} \right)^2 + h_{55} \left(\frac{\partial \hat{\Psi}}{\partial \overline{I}_5} \right)^2 + h_{12} \frac{\partial \hat{\Psi}}{\partial \overline{I}_1} \frac{\partial \hat{\Psi}}{\partial \overline{I}_2} + h_{15} \frac{\partial \hat{\Psi}}{\partial \overline{I}_1} \frac{\partial \hat{\Psi}}{\partial \overline{I}_5} \\ &+ h_{25} \frac{\partial \hat{\Psi}}{\partial \overline{I}_2} \frac{\partial \hat{\Psi}}{\partial \overline{I}_5}, \end{aligned} \tag{118}$$

where the coefficients h_{ij} are involved functions of the invariants, which, as explained in the main body of the text, turn out to be irrelevant to the problem at hand and are therefore omitted.

References

1. Honeker CC, Thomas EL (1996) Impact of morphological orientation in determining mechanical properties in triblock copolymers. Chem Mater 8:1702–1714
2. Honeker CC, Thomas EL, Albalak RJ, Hadjuk DA, Gruner SM, Capel MC (2000) Perpendicular deformation of a near–single crystal triblock copolymer with a cylindrical morphology. 1. Synchroton SAXS. Macromolecules 33:9395–9406
3. Finlay HM, Whittaker P, Canham PB (1998) Collagen organization in branching region of human brain arteries. Stroke 29:1595–1601
4. Quapp KM, Weiss JA (1998) Material characterization of human medial collateral ligament. J Biomech Eng 120:757–763
5. Spencer AJM (1972) Deformations of fibre-reinforced materials. Oxford University Press, Oxford
6. Triantafyllidis N, Abeyaratne RC (1983) Instability of a finitely deformed fiber-reinforced elastic material. J Appl Mech 50:149–156
7. Qiu GY, Pence TJ (1997) Remarks on the behavior of simple directionally reinforced incompressible nonlinearly elastic solids. J Elast 49:1–30
8. Merodio J, Ogden RW (2005) Mechanical response of fiber-reinforced incompressible nonlinear elastic solids. Int J Nonlinear Mech 40:213–227
9. Horgan CO, Saccomandi G (2005) A new constitutive theory for fiber-reinforced incompressible nonlinearly elastic solids. J Mech Phys Solids 53:1985–2015
10. Spencer AJM (1984) Continuum theory of the mechanics of fibre-reinforced composites. Springer, Wein, New York
11. Lopez-Pamies O, Ponte Castañeda P (2006) On the overall behavior, microstructure evolution, and macroscopic stability in reinforced rubbers at large deformations: II—application to cylindrical fibers. J Mech Phys Solids 54:831–863
12. deBotton G, Hariton I, Socolsky EA (2006) Neo-Hookean fiber-reinforced composites in finite elasticity. J Mech Phys Solids 54:533–559
13. Brun M, Lopez-Pamies O, Ponte Castañeda P (2007) Homogenization estimates for fiber-reiforced elastomers with periodic microstructures. Int J Solids Struct 44:5953–5979
14. Agoras M, Lopez-Pamies O, Ponte Castañeda P (2009) A general hyperelastic model for incompressible fiber-reinforced elastomers. J Mech Phys Solids 57:268–286
15. Idiart MI (2008) Modeling the macroscopic behavior of two-phase nonlinear composites by infinite-rank laminates. J Mech Phys Solids 56:2599–2617
16. deBotton G (2005) Transversely isotropic sequentially laminated composites in finite elasticity. J Mech Phys Solids 53:1334–1361
17. Lopez-Pamies O (2006) On the effective behavior, microstructure evolution, and macroscopic stability of elastomeric composites. Ph.D. Dissertation, University of Pennsylvania, USA
18. Willis JR (1982) Elasticity theory of composites. In: Hopkins HG, Sewell MJ (eds) Mechanics of solids, The Rodney Hill 60th anniversary volume. Pergamon Press, Oxford, pp 653–686
19. Hill R (1972) On constitutive macrovariables for heterogeneous solids at finite strain. Proc R Soc Lond A 326:131–147
20. Geymonat G, Müller S, Triantafyllidis N (1993) Homogenization of nonlinearly elastic materials, microscopic bifurcation and macroscopic loss of rank-one convexity. Arch Ration Mech Anal 122:231–290
21. Triantafyllidis N, Nestorovic MD, Schaard MW (2006) Failure surfaces for finitely strained two-phase periodic solids under general in-plane loading. J Appl Mech 73:505–516
22. Michel JC, Lopez-Pamies O, Ponte Castañeda P, Triantafyllidis N (2007) Microscopic and macroscopic instabilities in finitely strained porous elastomers. J Mech Phys Solids 55:900–938
23. Michel JC, Lopez-Pamies O, Ponte Castañeda P, Triantafyllidis N (2010) Microscopic and macroscopic instabilities in finitely strained particle-reinforced elastomers (submitted)
24. Lopez-Pamies O, Ponte Castañeda P (2009) Microstructure evolution in hyperelastic laminates and implications for overall behavior and macroscopic stability. Mech Mater 41:364–374
25. Hashin Z (1985) Large isotropic elastic deformation of composites and porous media. Int J Solids Struct 21:711–720
26. Bruggerman DAG (1935) Berechnung verschiedener physikalischer Konstanten von heterogenen Substanzen. I. Dielektrizittskonstanten und Leitfhigkeiten der Mischkrper aus isotropen Substanzen (German) [Calculation of various physical constants in heterogeneous substances. I. Dielectric constants and conductivity of composites from isotropic substances]. Ann Phys 416:636–664
27. Milton G (2002) The theory of composites. Cambridge University Press, Cambridge, UK
28. Duva JM (1984) A self-consistent analysis of the stiffening effect of rigid inclusions on a power-law material. ASME J Eng Mater Technol 106:317–321
29. Lopez-Pamies O (2010) An exact result for the macroscopic response of particle-reinforced Neo-Hookean solids. J Appl Mech 77:021016-1–021016-5
30. Eshelby JD (1957) The determination of the elastic field of an ellipsoidal inclusion and related problems. Proc R Soc Lond A 241:376–396
31. Lopez-Pamies O, Ponte Castañeda P (2006) On the overall behavior, microstructure evolution, and macroscopic stability in reinforced rubbers at large deformation: I—theory. J Mech Phys Solids 54:807–830
32. Lopez-Pamies O (2009) Onset of cavitation in compressible, isotropic, hyperelastic solids. J Elast 94:115–145

33. Triantafyllidis N, Maker BN (1985) On the comparison between microscopic and macroscopic instability mechanisms in a class of fiber-reinforced composites. J Appl Mech 52:794–800
34. Nesterovic N, Triantafyllidis N (2004) Onset of failure in finitely strained layered composites subjected to combined normal and shear loading. J Mech Phys Solids 52:941–974
35. Bourdin B, Kohn R (2008) Optimization of structural topology in the high-porosity regime. J Mech Phys Solids 56:1043–1064
36. Willis JR (1977) Bounds and self-consistent estimates for the overall moduli of anisotropic composites. J Mech Phys Solids 25:185–202
37. Polyanin AD, Zaitsev VF, Moussiaux A (2002) Handbook of first order partial differential equations. Taylor & Francis, London
38. Ponte Castañeda P, Willis JR (1995) The effect of spatial distribution on the effective behavior of composite materials and cracked media. J Mech Phys Solids 43:1919–1951
39. McLaughlin R (1977) A study of the differential scheme for composite materials. Int J Eng Sci 15:237–244
40. Ogden R (1978) Extremum principles in non-linear elasticity and theirapplication to composites—I Theory Int J Solids Struct. 14:265–282
41. He QC, Le Quang H, Feng ZQ (2006) Exact results for the homogenization of elastic fiber-reinforced solids at finite strain. J Elast 83:153–177
42. Idiart MI, Lopez-Pamies O (2010) Two-phase hyperelastic composites: a realizable homogenization constitutive theory (in preparation)
43. Idiart MI, Ponte Castañeda P (2007) Field statistics in nonlinear composites. I Theory Proc R Soc Lond A 463:183–202
44. Merodio J, Ogden RW (2003) Instabilities and loss of ellipticity in fiber-reinforced nonlinearly elastic solids under plane deformation. Int J Solids Struct 40:4707–4727
45. Lipton R (1992) Characterization of bounds and perturbation series for transversely isotropic, incompressible elastic composites. J Elast 27:193–225
46. Milton GW (1986) Modeling the properties of composites by laminates. In: Ericksen JL, Kinderlehrer D, Kohn R, Lions J-L (eds) Homogenization and effective moduli of materials and media, The IMA volumes in mathematics and its applications, vol 1. Springer, Berlin, pp 150–174
47. Moraleda J, Segurado J, Llorca J (2009) Finite deformation of incompressible fiber-reinforced elastomers: a computational micromechanics approach. J Mech Phys Solids. doi:10.1016/j.jmps.2009.05.007
48. Benton SH (1977) The Hamilton–Jacobi equation: a global approach. Mathematics in Science and Engineering, vol 131. Academic Press, New York
49. Ericksen JL, Rivlin RS (1954) Large elastic deformations of homogeneous anisotropic materials. J Ration Mech Anal 3:281–301